Journal of Intelligent Material Systems and Structures

Original Article

Journal of Intelligent Material Systems and Structures
2018, Vol. 29(13) 2840–2860

DOI: 10.1177/1045389X18781024
journals.sagepub.com/home/jim
SAGE

Analysis of a multi-axial quantum-informed ferroelectric continuum model: Part 2—sensitivity analysis

Lider Leon[1], Ralph C Smith[1], William S Oates[2] and Paul Miles[2]

Abstract

We illustrate the use of global sensitivity analysis, and a parameter subset selection algorithm based on local sensitivity analysis, to quantify the relative influence of parameters in polarization and electrostrictive energy relations for a quantum-informed, single-domain, ferroelectric material model. A motivating objective is to determine which parameters are identifiable or influential in the sense that they are uniquely determined by density functional theory–generated data. Noninfluential parameters will be fixed at nominal values for subsequent Bayesian inference, uncertainty propagation, and material design since variations in these parameters are minimally reflected in responses. Whereas global sensitivity analysis is typically based on the assumption of mutually independent, uniformly distributed parameters, we demonstrate that inherent parameter correlations must be accommodated to achieve correct interpretations of parameter influence. For the considered energy functionals, we demonstrate that all of the parameters are influential and will be informed by density functional theory–simulated data.

Keywords

Ferroelectric, density functional theory, Landau energy, sensitivity analysis

Introduction

Ferroelectric materials, such as lead zirconate titanate (PZT), have been widely employed as sensors and actuators due to their strong electromechanical coupling, relatively large work densities, fast actuation rates, and high setpoint accuracy. Due to the electromechanical coupling, they provide unique solid-state transducer capabilities that have the potential for simplifying and significantly improving the mechanical capabilities and energy efficiency of traditional mechatronic devices. Due to these attributes, ferroelectric materials have been considered or employed for high-speed valves for fuel injection, energy-harvesting circuits (Song et al., 2010), structural health monitoring sensors (Park et al., 2017), flow control transducers (Bilgen et al., 2011; Kumar et al., 2011), flying and ambulatory microrobots (Hoffman and Wood, 2011; Pérez-Arancibia et al., 2011; Wood, 2008; Wood et al., 2011), and ferroelectric memory technologies (e.g. FeRAM) (Scott, 2000). Additional discussion of applications can be found in the works by Cattafesta and Sheplak (2011), Chopra and Sirohi (2014), Jaffe et al. (1971), Leo (2007), Nuffer and Bein (2006), Smith and Hu (2012), Smith (2005), Uchino (2010), Uchino and Giniewicz (2003), and Vasic et al. (2004).

Despite their successes in smart and adaptive structures, there is significant research focused on multiscale and multiphysics analysis of ferroelectric materials from atomic to macroscopic scales. One motivation for this multiscale analysis is the need to better characterize and optimize the capabilities and performance of existing materials such as PZT. For example, physics-based quantification of the atomic properties that produce hysteresis and rate dependencies such as creep can be exploited to improve device designs and model-based control algorithms. A second, broader, objective is the goal of engineering materials at atomic scales to

[1]Department of Mathematics, North Carolina State University, Raleigh, NC, USA
[2]Florida Center for Advanced Aero-Propulsion (FCAAP), Department of Mechanical Engineering, Florida A&M University and Florida State University, Tallahassee, FL, USA

Corresponding author:
Ralph C Smith, Department of Mathematics, North Carolina State University, Raleigh, NC 27695, USA.
Email: rsmith@ncsu.edu

improve macroscale properties and capabilities. For example, there is significant research focused on developing lead-free materials whose performance is close to lead-based compounds but that are environmentally safe and feasible for biomedical applications.

In the companion manuscript (Miles et al., 2018), we detail the use of density functional theory (DFT) to quantify the atomic structure properties of lead titanate. These computations can be directly extended to lead zirconate and other perovskite single-crystal materials. Moreover, we anticipate that by exploiting mixtures of the two, we can simulate the electronic and structural properties of PZT. This provides us with the capability to generate simulated atomic-level data to inform continuum energy relations. However, scaling up electronic and atomic structure calculations into a continuum model leads to model uncertainties that may have significantly different parameter uncertainties.

As detailed in Miles et al. (2018), we employ classical functionals for the Landau polarization energy, electrostrictive energy, and mechanical energy. All of these relations contain phenomenological parameters that govern attributes of the energy behavior. For example, the sixth-order Landau polarization energy

$$\begin{aligned} u_P(\mathbf{P}) = {} & \alpha_1\left(P_1^2 + P_2^2 + P_3^2\right) + \alpha_{11}\left(P_1^2 + P_2^2 + P_3^2\right)^2 \\ & + \alpha_{12}\left(P_1^2P_2^2 + P_2^2P_3^2 + P_1^2P_3^2\right) \\ & + \alpha_{111}\left(P_1^6 + P_2^6 + P_3^6\right) \\ & + \alpha_{112}\left[P_1^4\left(P_2^2 + P_3^2\right) + P_2^4\left(P_1^2 + P_3^2\right)\right. \\ & \left. + P_3^4\left(P_1^2 + P_2^2\right)\right] + \alpha_{123}P_1^2P_2^2P_3^2 \end{aligned} \tag{1}$$

contains the parameters $\theta_P = [\alpha_1, \alpha_{11}, \alpha_{12}, \alpha_{111}, \alpha_{112}, \alpha_{123}]$ that specify the non-convex energy potential as a function of the polarization $\mathbf{P} = [P_1, P_2, P_3]$.

There are two fundamental questions pertaining to these parameters: (1) which of the parameters are identifiable or influential in the sense that they uniquely contribute to energy responses and (2) what are the actual parameter values that dictate the behavior of a specific material and what are the associated uncertainties in these values? The first comprises the sensitivity analysis detailed in this article. For the polarization relation (1), we will employ sensitivity analysis to ascertain whether the sixth-order model is necessary or whether a fourth-order model will suffice to approximate quantum calculations. The second question can be addressed through frequentist or Bayesian inference, and we address the latter using DFT-generated data in Miles et al. (2018).

To detail the role of sensitivity analysis, it is first necessary to define identifiable and influential parameter spaces. We consider the nonlinear input–output relation

$$y = f(\theta) \tag{2}$$

where $\theta = [\theta_1, \ldots, \theta_p]$ are model parameters, f denotes the mathematical model, and $y \in \mathbb{R}^1$ is a real-valued response. For the polarization energy (1), $\theta = \theta_P$ are the phenomenological parameters, f is the sixth-order relation, and $y = u_P(\mathbf{P})$ is the energy for a specified polarization value.

The concept of *identifiability* is classical and can be defined as follows. The parameters $\theta = [\theta_1, \ldots, \theta_p]$ are identifiable at θ^* if $f(\theta) = f(\theta^*)$ implies that $\theta = \theta^*$ for all admissible $\theta \in \mathbb{Q}$. The parameters θ are identifiable with respect to a space $I(\theta)$, termed the identifiable subspace, if this holds for all $\theta^* \in I(\theta)$. The unidentifiable parameter space $NI(\theta)$ is the orthogonal complement of $I(\theta)$ with regard to the admissible parameter space $\mathbb{Q}$ with the Euclidean inner product. Identifiable parameters can be uniquely determined from observations, whereas unidentifiable parameters must be fixed during model calibration using outputs y. An example of identifiable and unidentifiable parameters is illustrated in Figure 1(a) and (b), respectively.

Influential parameter spaces are sometimes defined differently in various disciplines. We define the parameters $\theta = [\theta_1, \ldots, \theta_p]$ to be *noninfluential* on the space $\mathcal{NI}(\theta)$ if $|f(\theta) - f(\theta^*)| < \varepsilon$ for all θ and $\theta^* \in \mathcal{NI}(\theta)$. The space of influential parameters, $\mathcal{I}(\theta)$, is defined to be the orthogonal component of $\mathcal{NI}(\theta)$ with respect to $\mathbb{Q}$. Noninfluential parameters, like unidentifiable parameters, can be fixed for model calibration and uncertainty propagation. An example of a noninfluential parameter is illustrated in Figure 1(c).

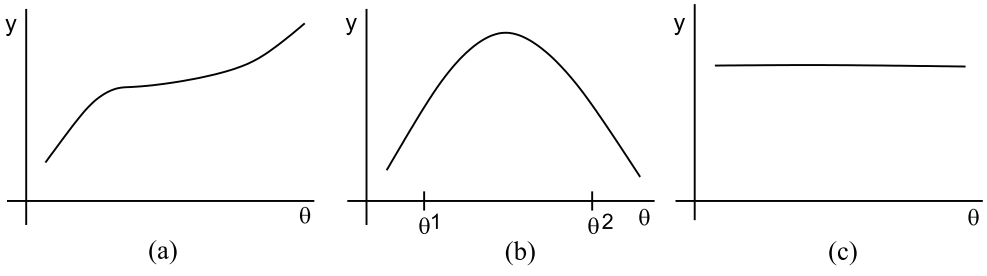

Figure 1. Illustration of $y = f(\theta)$ for (a) identifiable, (b) unidentifiable, and (c) noninfluential parameters θ.

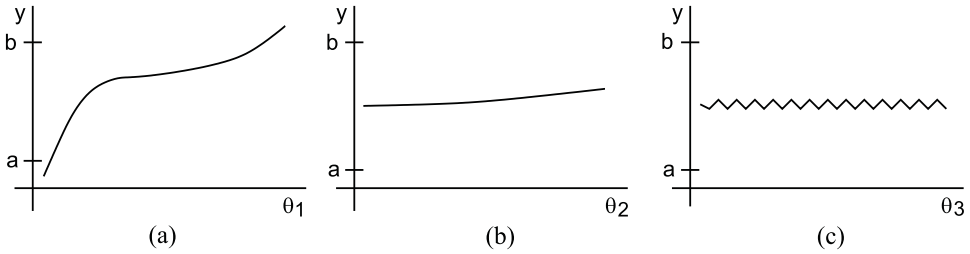

Figure 2. Illustration of (a) a highly influential parameter θ_1 and (b) minimally influential parameter θ_2. (c) Minimally influential parameter θ_3 having large local derivative values.

A parameter θ_1 is considered more influential than parameter θ_2 if changes in θ_1 produce greater changes in y than changes produced by θ_2 when both are considered over the admissible parameter space. In Figure 2(a) and (b), we illustrate highly and minimally influential parameters.

We note that noninfluential or unidentifiable parameter spaces can include individual parameters or linear or nonlinear combinations of parameters. To illustrate, consider the parameters $\theta = [\theta_1, \theta_2]$ in the admissible space $\mathbb{Q} = \mathbb{R}^2$ and the models $y = \theta_1$ and $y = \theta_1 - \theta_2$. For the first model, $NI(\theta) = \mathcal{NI}(\theta) = \{\theta_2 \in \mathbb{R}\}$, whereas $NI(\theta) = \mathcal{NI}(\theta) = \{(\theta_1, \theta_2) \in \mathbb{R}^2 | \theta_1 = \theta_2\}$ for the second. We focus on the first case in this article and note that active subspace methods can be employed for the second (Bang et al., 2012; Constantine, 2015).

From Figure 1(b) and (c), one observes that unidentifiable or noninfluential parameters can be *partially* characterized by the property that the local derivatives satisfy

$$\frac{\partial f}{\partial \theta_i}(\theta^*) = 0 \tag{3}$$

when evaluated at nominal values θ^*. Moreover, Figure 2(a) and (b) indicates that the magnitudes of local derivatives can be used to quantify the relative influence of parameters. This motivates the use of local sensitivity analysis and Fisher information matrices based on equation (3).

There are three difficulties associated with using the local derivative behavior to quantify parameter sensitivity. The first is that derivative values are typically unavailable unless models are sufficiently simple that they can be analytically differentiated—as is the case for the energy relations in this investigation—or codes have adjoint capabilities or associated sensitivity equations. This can often be addressed using finite-difference approximations, although approximation can degrade the accuracy of sensitivity measures. This is also the basis for certain screening methods, such as Morris screening (Cropp and Braddock, 2002; Morris, 1991; Smith, 2014), which statistically averages derivative approximations.

Of more serious consequence is the fact that equation (3) is local in nature and does not incorporate variability throughout the admissible parameter space. The parameter θ_3 depicted in Figure 2(c) is noninfluential but has large derivatives at certain nominal values due to high-frequency chatter. This is also partially addressed by Morris screening through statistically averaging at multiple nominal values.

Finally, local sensitivity analysis does not accommodate potential input and output uncertainties of the nature illustrated in the works by Saltelli et al. (2004, 2006, 2008, 2010) and Smith (2014). Specifically, it does not quantify the manner in which output uncertainties can be apportioned to input uncertainties as quantified by global sensitivity analysis.

To address these issues, we employ global sensitivity analysis in this investigation, which broadly quantifies how uncertainties in responses are apportioned to uncertainties in inputs (Saltelli et al., 2004, 2008; Smith, 2014). We focus on Sobol' analysis (Sobol', 1993, 2001; Sobol' et al., 2001), which is based on analysis of variance (ANOVA), but note that Morris screening is widely employed due to its computational efficiency.

When performing sensitivity analysis, one usually does not have a prior knowledge of the underlying parameter distribution. To avoid introducing unintentional biases, one typically assumes in such cases that parameters are mutually independent and uniformly distributed. As we will demonstrate using the Bayesian inference in Part 1 of these papers (Miles et al., 2018), parameters in the considered models are highly correlated and hence this assumption is false; for example, α_1 and α_{11} are negatively correlated in equation (1). We will additionally demonstrate that sensitivity analysis based on this false assumption yields incorrect interpretations about which parameters can be fixed during Bayesian inference. To illustrate these potential pitfalls, we present uncertainty analysis in Part 1 and sensitivity analysis in Part 2, whereas this ordering would typically be reversed when analyzing large-scale problems. We summarize in the "Concluding Remarks" section the manner in which sensitivity analysis can be addressed prior to Bayesian inference when parameter correlation is suspected.

We summarize in the section "Energy relations" the employed continuum energy relations in addition to the Landau energy in equation (1), the pertinent

parameters, and the formulation of scalar-valued pseudoresponses y based on vector-valued polarization, normal stress, and shear stress responses. In "Global sensitivity analysis and the fisher information matrix," we detail Sobol'-based global sensitivity analysis for correlated and independent parameters and construction of the Fisher information matrix, which is based on local sensitivities $(\partial f/\partial\theta)(\theta^*)$. In the "Results" section on "Global sensitivity analysis," we use Sobol' indices for the correlated parameters to indicate that all are influential and demonstrate in "Global sensitivity analysis: assumption of independent parameters" that analysis based on the incorrect assumption of mutually independent parameters yields false conclusions about potentially noninfluential parameters. Finally, we demonstrate in "Local identifiability analysis based on the Fisher information matrix" that identifiability analysis based on the Fisher information matrix corroborates the earlier global sensitivity analysis.

Energy relations

As detailed in Miles et al. (2018), we take polarization to be the order parameter. The stored energy per unit volume, expressed as a function of total strain $\boldsymbol{\varepsilon}$ and polarization $\mathbf{P}$, is

$$u(\boldsymbol{\varepsilon},\mathbf{P}) = u_M(\boldsymbol{\varepsilon}) + u_P(\mathbf{P}) + u_C(\boldsymbol{\varepsilon},\mathbf{P}) + u_R(\boldsymbol{\varepsilon}) \tag{4}$$

Here, $u(\boldsymbol{\varepsilon},\mathbf{P})$ is the total energy per unit volume, and u_M, u_P, u_C, and u_R, respectively, denote the strain, Landau, electrostrictive, and residual energy per unit volume. We denote the independent strain and polarization variables by $\boldsymbol{\varepsilon}$ and $\mathbf{P}$, respectively.

Based on the assumption of linear elasticity, the mechanical energy, with respect to a reference cubic state, is

$$\begin{aligned} u_M(\boldsymbol{\varepsilon}) = {} & \frac{c_{11}}{2}\left(\varepsilon_{11}^2 + \varepsilon_{22}^2 + \varepsilon_{33}^2\right) \\ & + c_{12}(\varepsilon_{11}\varepsilon_{22} + \varepsilon_{22}\varepsilon_{33} + \varepsilon_{11}\varepsilon_{33}) \\ & + 2c_{44}\left(\varepsilon_{12}^2 + \varepsilon_{23}^2 + \varepsilon_{13}^2\right) \end{aligned} \tag{5}$$

Here, c_{11}, c_{12}, and c_{44} are elastic coefficients expressed in Voigt notation (Malvern, 1969).

The sixth-order Landau polarization energy is

$$\begin{aligned} u_P(P) = {} & \alpha_1\left(P_1^2 + P_2^2 + P_3^2\right) + \alpha_{11}\left(P_1^2 + P_2^2 + P_3^2\right)^2 \\ & + \alpha_{12}\left(P_1^2P_2^2 + P_2^2P_3^2 + P_1^2P_3^2\right) \\ & + \alpha_{111}\left(P_1^6 + P_2^6 + P_3^6\right) \\ & + \alpha_{112}\left[P_1^4\left(P_2^2 + P_3^2\right) + P_2^4\left(P_1^2 + P_3^2\right)\right. \\ & \left. + P_3^4\left(P_1^2 + P_2^2\right)\right] + \alpha_{123}P_1^2P_2^2P_3^2 \end{aligned} \tag{6}$$

where $\alpha_1, \alpha_{11}, \alpha_{12}, \alpha_{111}, \alpha_{112}$ and α_{123} are phenomenological parameters. One goal of sensitivity and uncertainty analysis is to determine the necessity of including sixth-order terms rather than employing a fourth-order relation.

The electrostrictive energy is

$$\begin{aligned} u_C(\boldsymbol{\varepsilon},\mathbf{P}) = {} & -q_{11}\left(\varepsilon_{11}P_1^2 + \varepsilon_{22}P_2^2 + \varepsilon_{33}P_3^2\right) \\ & - q_{12}\left[\varepsilon_{11}\left(P_2^2 + P_3^2\right)\right. \\ & \left. + \varepsilon_{22}\left(P_1^2 + P_3^2\right) + \varepsilon_{33}\left(P_1^2 + P_2^2\right)\right] \\ & - 4q_{44}(\varepsilon_{12}P_1P_2 + \varepsilon_{13}P_1P_3 + \varepsilon_{23}P_2P_3) \end{aligned} \tag{7}$$

where q_{11}, q_{12}, and q_{44} denote the electrostrictive coefficients.

The residual energy

$$u_R(\boldsymbol{\varepsilon}) = \sigma_{ij}^R\varepsilon_{ij} \tag{8}$$

arises since the unit cell is held fixed with respect to the reference cubic state. Hence, the unknown required residual stress σ_{ij}^R constrains the unit cell to the cubic state.

We next summarize the parameters, independent variables, and responses used in Miles et al. (2018) to employ DFT analysis to calibrate the monodomain continuum model. This forms the basis for the global sensitivity analysis detailed in this article.

Monodomain continuum model

In the DFT analysis detailed in Miles et al. (2018), we focus on energy, stress, and polarization computations. We hold the unit cell fixed so that the total strain is zero in the cubic state. This permits the polarization energy (equation (6)) to be calibrated to DFT computations independent of electrostrictive coupling due to equation (7). The additional effect of electrostriction is incorporated by evaluating the continuum stress

$$\boldsymbol{\sigma} = \frac{\partial u}{\partial \boldsymbol{\varepsilon}} \tag{9}$$

This yields the stress tensor

$$\boldsymbol{\sigma} = \mathbf{c} : \boldsymbol{\varepsilon} + \boldsymbol{\sigma}^R - \mathbf{q} : \mathbf{PP} \tag{10}$$

where $\mathbf{c}$ is the fourth-order elastic tensor and $\boldsymbol{\sigma}^R$ is the residual stress tensor obtained from the derivative of the residual energy (equation (8)) with respect to strain.

In the following expanded equations, we employ the Einstein summation convention in which one sums over repeated indices. The tensor indices are reduced to Voigt notation using the convention $()_{11} \to ()_1$, $()_{22} \to ()_2$, $()_{33} \to ()_3$, $()_{23} \to ()_4$, $()_{13} \to ()_5$ and $()_{12} \to ()_6$. This notation is applied to the elastic and electrostrictive coefficients.

To simplify DFT computations, we constrain the polarization to move from P_3 to P_2, with employed values shown in Figure 3. It follows that $\sigma_{11}^R = \sigma_{22}^R$ and $\sigma_{12}^R = \sigma_{13}^R = 0$. The remaining stress components are

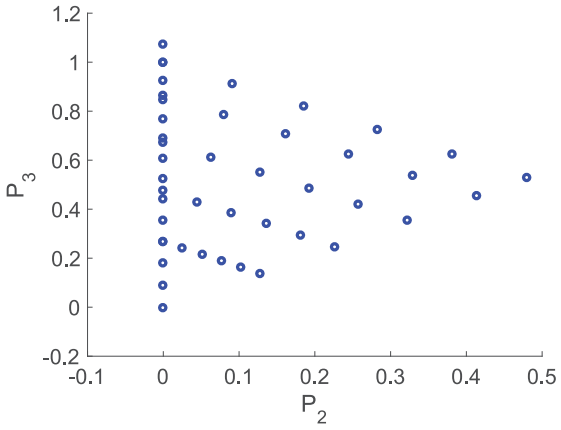

Figure 3. Input values of P_2 and P_3 for equation (15).

$$\begin{aligned}\sigma_{11} &= c_{11}\varepsilon_{11} + c_{12}(\varepsilon_{22} + \varepsilon_{33}) \\ &\quad - q_{11}P_1^2 - q_{12}\left(P_2^2 + P_3^2\right) + \sigma_{11}^R \\ \sigma_{22} &= c_{11}\varepsilon_{22} + c_{12}(\varepsilon_{11} + \varepsilon_{33}) \\ &\quad - q_{11}P_2^2 - q_{12}\left(P_1^2 + P_3^2\right) + \sigma_{22}^R \\ \sigma_{33} &= c_{11}\varepsilon_{33} + c_{12}(\varepsilon_{11} + \varepsilon_{22}) \\ &\quad - q_{11}P_3^2 - q_{12}\left(P_1^2 + P_2^2\right) + \sigma_{33}^R \\ \sigma_{23} &= 2c_{44}\varepsilon_{23} - 2q_{44}P_2P_3 + \sigma_{23}^R\end{aligned} \tag{11}$$

Since the elastic properties of lead titanate are well-understood, we assume fixed elastic properties from previous DFT simulations (King-Smith and Vanderbilt, 1994) and neglect uncertainty and sensitivity with respect to the elastic coefficients c_{11}, c_{12}, and c_{44}. We evaluate sensitivities with respect to the zero strain case.

The polarization energy parameters are

$$\theta_P = [\alpha_1, \alpha_{11}, \alpha_{12}, \alpha_{111}, \alpha_{112}] \tag{12}$$

and the normal and shear stress coefficients are, respectively

$$\theta_{\sigma_{ns}} = \left[q_{11}, q_{12}, \sigma_{11}^R, \sigma_{22}^R, \sigma_{33}^R\right],\ \theta_{\sigma_s} = \left[q_{44}, \sigma_{23}^R\right] \tag{13}$$

The combined set of stress component parameters is thus

$$\theta_\sigma = [\theta_{\sigma_{ns}}, \theta_{\sigma_s}]$$

and the monodomain model parameters are

$$\theta_{MD} = [\theta_P, \theta_\sigma] \tag{14}$$

The DFT outputs, or responses, are

$$y_{MD}(\theta_{MD}) = [u_P(\theta_P), \sigma_{11}(\theta_{\sigma_{ns}}), \sigma_{22}(\theta_{\sigma_{ns}}), \sigma_{33}(\theta_{\sigma_{ns}}), \sigma_{23}(\theta_{\sigma_s})] \tag{15}$$

which include the Landau polarization energy and the normal and shear stresses. We note that while all are functions of the polarization, we suppress this dependence when discussing the sensitivity of responses to parameters. In addition, the sensitivity of these responses to the polarization energy parameters θ_P and stress parameters θ_σ can be analyzed separately due to the independence between $u_P(\theta_P)$ and $\sigma_{11}(\theta_{\sigma_{ns}})$, $\sigma_{22}(\theta_{\sigma_{ns}})$, $\sigma_{33}(\theta_{\sigma_{ns}})$, $\sigma_{23}(\theta_{\sigma_s})$.

For standard global sensitivity analysis, it is necessary to construct scalar-valued responses of the parameters θ_P, $\theta_{\sigma_{ns}}$, and θ_σ and polarization values (P_2^n, P_3^n), which serve as independent variables.

For the polarization energy response u_P defined in equation (6), we employ the pseudoresponse

$$Y_P(\theta_P) = \frac{1}{N}\sum_{n=1}^{N} u_P\left(P_2^n, P_3^n; \theta_P\right) \tag{16}$$

which averages over the N polarization values (P_2^n, P_3^n), $n = 1, \ldots, N$, plotted in Figure 3. For the vector-valued stress responses $y_{\sigma_{ns}}(\theta_{\sigma_{ns}}) = [\sigma_{11}, \sigma_{22}, \sigma_{33}]$ and $y_{\sigma_s}(\theta_{\sigma_s}) = \sigma_{23}$, where $\sigma_{11}, \sigma_{22}, \sigma_{33}$, and σ_{23} are defined in equation (11), we construct the pseudoresponses

$$\begin{aligned}Y_{\sigma_{ns}}(\theta_{\sigma_{ns}}) &= \frac{1}{3N}\sum_{n=1}^{N} \sigma_{11}\left(P_2^n, P_3^n; \theta_{\sigma_{ns}}\right) \\ &\quad + \frac{1}{3N}\sum_{n=1}^{N} \sigma_{22}\left(P_2^n, P_3^n; \theta_{\sigma_{ns}}\right) \\ &\quad + \frac{1}{N}\sum_{n=1}^{N} \sigma_{33}\left(P_2^n, P_3^n; \theta_{\sigma_{ns}}\right)\end{aligned} \tag{17}$$

and

$$Y_{\sigma_s}(\theta_{\sigma_s}) = \frac{1}{N}\sum_{n=1}^{N} \sigma_{23}\left(P_2^n, P_3^n; \theta_{\sigma_s}\right) \tag{18}$$

The monodomain responses $Y_P(\theta_P)$, $Y_{\sigma_{ns}}(\theta_{\sigma_{ns}})$, and $Y_{\sigma_s}(\theta_{\sigma_s})$ in equations (16) to (18) are linearly parameterized so we can express them as

$$\begin{aligned}Y_P(\theta_P) &= [a_1\, a_2\, a_3\, a_4\, a_5][\alpha_1\, \alpha_{11}\, \alpha_{12}\, \alpha_{111}\, \alpha_{112}]^T \\ Y_{\sigma_{ns}}(\theta_{\sigma_{ns}}) &= [b_1\, b_2\, b_3\, b_4\, b_5][q_{11}\, q_{12}\, \sigma_{11}^R\, \sigma_{22}^R\, \sigma_{33}^R]^T \\ Y_{\sigma_s}(\theta_{\sigma_s}) &= [c_1\, c_2][q_{44}\, \sigma_{23}^R]^T\end{aligned}$$

where

$$a_1 = \frac{1}{N}\sum_{n=1}^{N}\left(P_{2_n}^2 + P_{3_n}^2\right),\ a_2 = \frac{1}{N}\sum_{n=1}^{N}\left(P_{2_n}^2 + P_{3_n}^2\right)^2$$

$$a_3 = \frac{1}{N}\sum_{n=1}^{N} P_{2_n}^2 P_{3_n}^2,\ a_4 = \frac{1}{N}\sum_{n=1}^{N}\left(P_{2_n}^6 + P_{3_n}^6\right)$$

$$a_5 = \frac{1}{N}\sum_{n=1}^{N}\left(P_{2_n}^4 P_{3_n}^2 + P_{3_n}^4 P_{2_n}^2\right)$$

and

$$b_1 = -\frac{1}{3N}\sum_{n=1}^{N}\left(P_{2_n}^2 + P_{3_n}^2\right)$$

$$b_2 = -\frac{2}{3N}\sum_{n=1}^{N}\left(P_{2_n}^2 + P_{3_n}^2\right)$$

$$b_3 = b_4 = b_5 = \frac{1}{3}$$

$$c_1 = -\frac{1}{N}\sum_{n=1}^{N}(P_{2_n}P_{3_n}),\ c_2 = 1$$

This facilitates the analytical determination of the component functions in the high-dimensional model representation (HDMR).

For global sensitivity analysis, we generically express equations (16) to (18) as

$$Y = f(\Theta) \tag{19}$$

Here, Y denotes the polarization response Y_P, the electrostrictive normal stress response $Y_{\sigma_{ns}}$ or the electrostrictive shear stress response Y_{σ_s}, and $\Theta = [\Theta_1, \ldots, \Theta_p]$ is Θ_P, $\Theta_{\sigma_{ns}}$, or Θ_{σ_s}. We employ Θ to represent random variables and θ to indicate realizations of those random variables.

Global sensitivity analysis and the Fisher information matrix

The objective of sensitivity analysis is to quantify the sensitivity of the responses $Y_P(\theta_P), Y_{\sigma_{ns}}(\theta_{\sigma_{ns}})$, and $Y_{\sigma_s}(\theta_{\sigma_s})$ in equations (16) to (18) to the parameters $\theta_P, \theta_{\sigma_{ns}}$, and θ_{σ_s}. In local sensitivity analysis, one approximates the derivatives of responses with respect to parameters and evaluates them at nominal parameter values, to quantify the influence of parameters on responses; that is, see equation (3). As detailed in Chapter 15 of Smith (2014), global sensitivity analysis more broadly quantifies how uncertainties in responses can be apportioned to uncertainties in parameters.

We employ both techniques to illustrate their relative merits. The objective is to determine whether any of the parameters θ_P, $\theta_{\sigma_{ns}}$, or θ_{σ_s} are unidentifiable or noninfluential, in the sense defined in the "Introduction," section and hence should be fixed for subsequent Bayesian inference and uncertainty quantification.

To avoid scaling issues, it is standard to first map sampled parameter values to the interval $[0, 1]$ using the cumulative distribution function (CDF) of the marginal probability density functions (PDFs) of Θ. Specifically, for a general parameter Θ, the parameter input space is mapped using the relation

$$r(\theta) = F(\theta) = \int_{-\infty}^{\theta} \rho_\Theta(\xi)d\xi \tag{20}$$

for realizations $\theta \in \mathbb{R}$, where $\rho_\Theta(\xi)$ is the PDF of Θ.

Sobol' indices

Sobol' indices for correlated parameters and general densities. We focus here on the input–output relation

$$Y = f(\Theta)$$

defined in equation (19), where Y is scalar-valued and $\Theta = [\Theta_1, \ldots, \Theta_p]$ has the joint density $\rho_\Theta(\theta)$. In the section on "Sobol' indices for independent parameters with uniform densities," we illustrate the special case of independent, uniformly distributed parameters.

To construct the global sensitivity indices, the model response for realizations θ is represented by the HDMR or Sobol' decomposition

$$\begin{aligned} f(\theta) &= f_0 + \sum_{i=1}^{p} f_i(\theta_i) + \sum_{1\le i<j\le p} f_{ij}(\theta_i,\theta_j) + \cdots \\ &\quad + f_{1,2,\ldots,p}(\theta_1, \ldots, \theta_p) \\ &= \sum_{\mathbf{i}'\subseteq\{1,\ldots,p\}} f_{\mathbf{i}'}(\theta_{\mathbf{i}'}) \end{aligned} \tag{21}$$

defined in the work by Sobol' (1993). The second representation utilizes the functional form detailed in the work by Smith (2014), where $\mathbf{i}' = \{i_1, \ldots, i_n\}$ comprises a set of integers with cardinality $n \le p$, $\theta_{\mathbf{i}'} = [\theta_{i_1}, \ldots, \theta_{i_n}]$, and $f_\emptyset \equiv f_0$. We note that each of the component functions is constructed to satisfy

$$\int_{\Gamma_{\mathbf{i}'}} \rho_{\mathbf{i}'}(\theta_{\mathbf{i}'}) f_{\mathbf{i}'}(\theta_{\mathbf{i}'})d\theta_{\mathbf{i}'} = 0 \tag{22}$$

to ensure that the component functions are uniquely defined. Here, $\rho_{\mathbf{i}'}(\theta_{\mathbf{i}'})$ is the joint PDF for the parameter set $\theta_{\mathbf{i}'}$. As detailed in the work by Smith (2014), the component functions can then be expressed as follows

$$\begin{aligned} f_0 &= \int_\Gamma \rho(\theta) f(\theta)d\theta = \mathbb{E}(Y) \\ f_i(\theta_i) &= \int_{\Gamma_{\sim i}} \rho_{\sim i}(\theta_{\sim i}) f(\theta)d\theta_{\sim i} - f_0 = \mathbb{E}(Y|\theta_i) - f_0 \\ f_{ij}(\theta_i,\theta_j) &= \int_{\Gamma_{\sim\{ij\}}} \rho_{\sim\{ij\}}(\theta_{\sim\{ij\}}) f(\theta)d\theta_{\sim\{ij\}} \\ &\quad - f_i(\theta_i) - f_j(\theta_j) - f_0 \\ &= \mathbb{E}[Y|q_i, q_j] - f_i(\theta_i) - f_j(\theta_j) - f_0 \\ f_{1\ldots p}(\theta_1, \ldots, \theta_p) &= f(\theta) - f_0 - \sum_{1\le i\le p} f_i(\theta_i) \\ &\quad - \sum_{1\le i<j\le p} f_{ij}(\theta_i,\theta_j) \\ &\quad - \sum_{1\le i<j<k\le p} f_{ijk}(\theta_i,\theta_j,\theta_k) - \cdots \end{aligned} \tag{23}$$

where Γ, $\Gamma_{\sim i}$, and $\Gamma_{\sim\{ij\}}$ are the image spaces for θ, $\theta_{\sim i} \equiv [\theta_1, \ldots, \theta_{i-1}, \theta_{i+1}, \ldots, \theta_p]$, and

$$\theta_{\sim\{ij\}} \equiv [\theta_1, \ldots, \theta_{i-1}, \theta_{i+1}, \ldots, \theta_{j-1}, \theta_{j+1}, \ldots, \theta_p]$$

Likewise, $\rho_{\sim i}(\theta_{\sim i})$ and $\rho_{\sim\{ij\}}(\theta_{\sim\{ij\}})$, respectively, denote the conditional PDFs for $\theta_{\sim i}$ and $\theta_{\sim\{ij\}}$ given θ_i and (θ_i, θ_j). To construct the sensitivity indices, we define the total and partial variances

$$\begin{aligned} D &= \int_{\Gamma} \rho(\theta) f^2(\theta) d\theta - f_0^2 = \mathrm{var}[Y] \\ D_i &= \int_{\Gamma_i} \rho_i(\theta_i) f_i^2(\theta_i) d\theta_i = \mathrm{var}[\mathbb{E}(Y|\theta_i)] \\ D_{ij} &= \int_{\Gamma_{ij}} \rho_{ij}(\theta_i, \theta_j) f_{ij}^2(\theta_i, \theta_j) d\theta_i d\theta_j \\ &= \mathrm{var}[\mathbb{E}(Y|\theta_i, \theta_j)] - \mathrm{var}[\mathbb{E}(Y|\theta_i)] - \mathrm{var}[\mathbb{E}(Y|\theta_j)] \\ &\vdots \end{aligned}$$

To account for correlations in the parameter structure of the component functions, we employ a formulation of $\mathrm{var}[Y]$ proposed in the work by Li et al. (2010). For general parameters θ, this derivation employs the Hilbert space inner product

$$\langle f(\theta), g(\theta) \rangle_\rho \equiv \int_{\Gamma} \rho(\theta) f(\theta) g(\theta) d\theta$$

to express $\mathrm{var}[Y]$ as

$$\begin{aligned} \mathrm{var}[Y] &= \mathbb{E}\left[(Y - \mathbb{E}[Y])^2 \right] \\ &= \langle y - f_0, y - f_0 \rangle_\rho = \left\langle \sum_{n=1}^{2^p - 1} f_{r_n}, y - f_0 \right\rangle_\rho \end{aligned}$$

Here, r_n, $1 \le n \le 2^p - 1$, represents all the possible sets $\{i | 1 \le i \le p\}$, $\{ij | 1 \le i < j \le p\}$, ... of parameter indices for the component functions, using the functional form in the work by Li et al. (2010). For example, letting $C_2^p = (p/2)$, the first- and second-order component functions are

$$\begin{aligned} &\text{1st order} : f_{r_1}(\theta_{r_1}) = f_1(\theta_1), \ldots, f_{r_p}(\theta_{r_p}) = f_p(\theta_p) \\ &\text{2nd order} : f_{r_{p+1}}(\theta_{r_{p+1}}) = f_{12}(\theta_1, \theta_2), \ldots, \\ &f_{r_{p + C_2^p}}\left(\theta_{r_{p + C_2^p}}\right) = f_{p-1,p}(\theta_{p-1}, \theta_p) \end{aligned}$$

The linearity of the inner product and relation (22) are then invoked to obtain the variance decomposition

$$\begin{aligned} \mathrm{var}[Y] &= \sum_{n=1}^{2^p - 1} \mathrm{cov}[f_{r_n}, Y] \\ &= \sum_{n=1}^{2^p - 1} \mathrm{var}[f_{r_n}] + \mathrm{cov}\left[f_{r_n}, \sum_{\ell = 1, \ell \neq n}^{2^p - 1} f_{r_\ell} \right] \end{aligned} \tag{24}$$

where

$$\begin{aligned} \mathrm{cov}[f_{r_n}, Y] &= \int_{\Gamma} \rho(\theta) f_{r_n}(\theta_{r_n}) [f(\theta) - f_0] d\theta \\ D_{r_n} &= \mathrm{var}[f_{r_n}] = \int_{\Gamma_{r_n}} \rho_{r_n}(\theta_{r_n}) f_{r_n}^2(\theta_{r_n}) d\theta_{r_n} \end{aligned} \tag{25}$$

The sensitivity indices are then defined to be

$$\begin{aligned} S_{r_n} &= \frac{\mathrm{cov}[f_{r_n}, Y]}{D}, \; S_{r_n}^s = \frac{D_{r_n}}{D} \\ S_{r_n}^c &= \frac{\mathrm{cov}[f_{r_n}, \sum f_{r_\ell}]}{D} \end{aligned} \tag{26}$$

where $S_{r_n} = S_{r_n}^s + S_{r_n}^c$. As detailed in the work by Li et al. (2010), $S_{r_n}^s$ and $S_{r_n}^s$, respectively, correspond to the structural and correlative contributions to the total index S_{r_n}. The indices (equation (26)) satisfy

$$\sum_{n=1}^{2^p - 1} S_{r_n} = 1$$

The integrals in the indices S_{r_n} and $S_{r_n}^s$ are approximated using Monte Carlo integration techniques (Li et al., 2010; Sobol', 2001), whereas the index $S_{r_n}^c$ is simply computed using the relation

$$S_{r_n}^c = S_{r_n} - S_{r_n}^s$$

In addition, we define the total sensitivity indices

$$S_{T_i} = S_i + \sum_{\substack{j=1 \\ j \neq i}}^{p} S_{ij} + \sum_{\substack{1 \le j < k \le p \\ j,k \neq i}} S_{ijk} + \cdots + S_{1,\ldots,p} \tag{27}$$

which quantify the total effect of the parameter θ_i on the response, including high-order structural interactions and correlative contributions.

When analyzing first-order Sobol' indices, a rough guide is to consider first-order Sobol' indices S_i that are greater than $(100/p)\%$ as significant because, in the absence of interactions, they have greater than average effect on the response variability. Higher-order Sobol' indices may be negative due to the correlations between the parameters. To measure the significance of any negative Sobol' indices, we consider the magnitude of the index as well as the value of the total index S_{T_i} (equation (27)).

Sobol' indices for independent parameters with uniform densities. For the special case when the parameters

$\Theta = [\Theta_1, \ldots, \Theta_p]$ are independent and uniformly distributed on the hypercube $\Gamma = [0,1]^p$—that is, $\Theta_i \sim \mathcal{U}(0,1)$ for $i = 1, \ldots, p$—one can significantly simplify the relations for the component functions f_0, f_i, f_{ij}, and Sobol' indices. As detailed in the works by Ma and Zabaras (2010), Rabitz and Alis (1999), Smith (2014), and Sobol' (1993), the component functions in this case are

$$\begin{aligned} f_0 &= \mathbb{E}[Y] = \int_{\Gamma} f(\theta) d\theta \\ f_i(\theta_i) &= \mathbb{E}[Y|\theta_i] - f_0 = \int_{\Gamma^{p-1}} f(\theta) d\theta_{\sim i} - f_0 \\ f_{ij}(\theta_i, \theta_j) &= \mathbb{E}\left[Y|\theta_i, \theta_j\right] - f_i(\theta_i) - f_j(\theta_j) - f_0 \\ &= \int_{\Gamma^{p-2}} f(\theta) d\theta_{\sim\{ij\}} - f_i(\theta_i) - f_j(\theta_j) - f_0 \\ &\vdots \end{aligned} \tag{28}$$

Here, $\Gamma^{p-1} = [0,1]^{p-1}$, $\Gamma^{p-2} = [0,1]^{p-2}$, ..., and $\theta_{\sim\{ij\}}$ denotes the vector having all components of θ except the ones corresponding to the subset $\{ij\}$; that is, $d\theta_{\sim i} = d\theta_1 \cdots d\theta_{i-1} d\theta_{i+1} \cdots d\theta_p$.

Since the parameters are assumed to be mutually independent, the second right-hand expression in equation (24) reduces to zero; that is

$$\operatorname{cov}\left[f_{r_n}, \sum_{\ell=1, \ell \neq n}^{2^p-1} f_{r_\ell}\right] = 0 \tag{29}$$

Hence, the component functions f_{r_n} are mutually orthogonal. Therefore, the correlative sensitivity index $S^c_{r_n}$ in equation (26) reduces to

$$S^c_{r_n} = \frac{\operatorname{cov}[f_{r_n}, \sum f_{r_\ell}]}{D} = 0 \tag{30}$$

This shows that there are no correlative contributions to the index S_{r_n} representing total contributions. The total contributions can then be expressed as follows

$$S_{r_n} = \frac{\operatorname{cov}[f_{r_n}, Y]}{D} = S^s_{r_n} = \frac{\operatorname{Var}[f_{r_n}]}{D} = \frac{D_{r_n}}{D} \tag{31}$$

That is, the sensitivity index representing the total contributions is equal to the index representing the structural contribution. Thus, one obtains the relation

$$S_{r_n} = \frac{D_{r_n}}{D} = \frac{\operatorname{var}[f_{r_n}]}{\operatorname{var}[Y]} = \frac{\int_{\Gamma^n} f^2_{r_n}(\theta_{r_n}) d\theta_{r_n}}{\int_{\Gamma} f^2(\theta) d\theta - f_0^2} \tag{32}$$

for the sensitivity index representing the total contribution from θ_{r_n}. Here, $\Gamma^n = [0,1]^n$ represents the input space for the set θ_{r_n}.

The integrals in equation (32) are approximated using Monte Carlo integration in a manner similar to the approximation to equation (26). When p is large, this becomes prohibitively expensive. For problems where $f(\theta)$ can be approximated by a second-order HDMR representation

$$f(\theta) = f_0 + \sum_{i=1}^{p} f_i(\theta_i) + \sum_{1 \le i < j \le p} f_{ij}(\theta_i, \theta_j) + \varepsilon$$

where $\varepsilon \sim \mathcal{N}(0, \sigma^2)$ represents truncation error, one obtains the Sobol' indices

$$\begin{aligned} S_i &= \frac{D_i}{D} = \frac{\operatorname{var}[\mathbb{E}(Y|\theta_i)]}{\operatorname{var}[Y]}, \; S_{ij} = \frac{D_{ij}}{D}, \quad i,j = 1, \ldots p \\ S_{T_i} &= S_i + \sum_{\substack{j=1 \\ i \neq j}}^{p} S_{ij} = 1 - \frac{\operatorname{var}[\mathbb{E}(Y|\theta_{\sim i})]}{\operatorname{var}[Y]} \end{aligned}$$

which satisfy

$$\sum_{i=1}^{p} S_i + \sum_{1 \le i < j \le p} S_{ij} = 1 \tag{33}$$

In this case, algorithms such as those proposed in the works by Saltelli (2002), Saltelli et al. (2010), Sobol' et al. (2001), and Weirs et al. (2012), can be used to construct estimators for the sensitivity indices. These algorithms greatly reduce the number of function evaluations otherwise required for Monte Carlo sampling–based quadrature. For example, for the polarization energy and normal stress parameter sets θ_P in equation (12) and $\theta_{\sigma_{ns}}$ in equation (13), the dimensions are $p = 5$, which makes Monte Carlo sampling–based quadrature over Γ^p, Γ^{p-1}, and Γ^{p-2} expensive. To address this, we employ Algorithm 3.1 as presented by Wentworth et al. (2016), to construct estimators for S_i and S_{T_i}.

Analytical computation for linearly parameterized problems

Consider linearly parameterized problems

$$Y = f(\Theta) = a_1\Theta_1 + a_2\Theta_2 + \cdots a_p\Theta_p \tag{39}$$

such as (16) for the monodomain model. We make the assumption that $\Theta \sim \mathcal{N}(\boldsymbol{\mu}, \mathbf{V})$ where $\boldsymbol{\mu} = [\mu_1, \mu_2, \ldots, \mu_p]^T$ is a vector of nominal values for Θ and $\mathbf{V}$ is the $p \times p$ corresponding covariance matrix. As before, we denote realizations of the random variable Θ by θ.

We construct the component functions (23) by evaluating conditional expected values in

Algorithm 3.1: Saltelli algorithm to compute first-order and total Sobol' sensitivity indices for uniform densities (Saltelli et al., 2010)

(1) For M Monte Carlo evaluations from $\mathcal{U}(I^p)$, create two $M \times p$ sample matrices

$$A = \begin{bmatrix} \theta_1^1 & \cdots & \theta_i^1 & \cdots & \theta_p^1 \\ \vdots & & \vdots & & \vdots \\ \theta_1^M & \cdots & \theta_i^M & \cdots & \theta_p^M \end{bmatrix}$$

$$B = \begin{bmatrix} \hat{\theta}_1^1 & \cdots & \hat{\theta}_i^1 & \cdots & \hat{\theta}_p^1 \\ \vdots & & \vdots & & \vdots \\ \hat{\theta}_1^M & \cdots & \hat{\theta}_i^M & \cdots & \hat{\theta}_p^M \end{bmatrix}$$

The entries of these matrices are pseudorandom numbers drawn from the respective density. In our investigation, the number of parameters is $p = 5$ for the polarization energy response $Y_P(\theta_P)$ (equation (16)), $p = 5$ for the normal stress response $Y_{\sigma_{ns}}(\theta_{\sigma_{ns}})$ (equation (17)), and $p = 2$ for the shear stress response $Y_{\sigma_s}(\theta_{\sigma_s})$ (equation (18)).

(2) Create

$$A_B^{(i)} = \begin{bmatrix} \theta_1^1 & \cdots & \hat{\theta}_i^1 & \cdots & \theta_p^1 \\ \vdots & & & & \\ \theta_1^M & \cdots & \hat{\theta}_i^M & \cdots & \theta_p^M \end{bmatrix} \tag{34}$$

where the entries are identical to A with the exception that the ith column is taken from B. Create $B_A^{(i)}$ in a similar manner.

(3) Create

$$C = \begin{bmatrix} A \\ -- \\ B \end{bmatrix} \tag{35}$$

which is the B matrix appended to matrix A.

(4) Compute the column vectors $f(A)$, $f(B)$, $f(A_B^{(i)})$, and $f(B_A^{(i)})$ by evaluating the model at input values from the rows of matrices A, B, $A_B^{(i)}$, and $B_A^{(i)}$. Here, $f(A)_j$ denotes the output computed from the jth row of A.

(5) The first-order Sobol' indices are estimated by

$$S_i \approx \frac{\frac{1}{M}\sum_{j=1}^{M}\left[f(A)_j f(B_A^{(i)})_j - f(A)_j f(B)_j\right]}{\frac{1}{2M}\sum_{j=1}^{2M} f(C)_j f(C)_j - \mathbb{E}^2[f(C)]} \tag{36}$$

and the total indices by

$$S_{T_i} \approx \frac{\frac{1}{2M}\sum_{j=1}^{M}\left[f(A)_j - f(A_B^{(i)})_j\right]^2}{\frac{1}{2M}\sum_{j=1}^{2M} f(C)_j f(C)_j - \mathbb{E}^2[f(C)]} \tag{37}$$

In equation (36), we approximated the squared mean

$$f_0^2 = \int_{I^p} f(\theta) f(\theta') d\theta d\theta'$$

by

$$f_0^2 \approx \frac{1}{M}\sum_{j=1}^{M} f(A)_j f(B)_j \tag{38}$$

as motivated in the works by Saltelli (2002) and Sobol' et al. (2001).

$$\begin{aligned} f_0 &= \mathbb{E}[Y] = \mathbb{E}\left[a_1\Theta_1 + a_2\Theta_2 + \cdots + a_p\Theta_p\right] \\ &= a_1\mathbb{E}[\Theta_1] + a_2\mathbb{E}[\Theta_2] + \cdots + a_p\mathbb{E}\left[\Theta_p\right] \\ &= a_1\mu_1 + \cdots + a_p\mu_p \\ f_i(\theta_i) &= \mathbb{E}[Y|\theta_i] - f_0 \\ &= a_1\mathbb{E}[\Theta_1|\theta_i] + \cdots + a_p\mathbb{E}\left[\Theta_p|\theta_i\right] - f_0, \\ f_{ij}(\theta_i,\theta_j) &= \mathbb{E}\left[Y|\theta_i,\theta_j\right] - f_i(\theta_i) - f_j(\theta_j) - f_0 \\ &= a_1\mathbb{E}\left[\Theta_1|\theta_i,\theta_j\right] + \cdots + a_p\mathbb{E}\left[\Theta_p|\theta_i,\theta_j\right] \\ &\quad - f_i(\theta_i) - f_j(\theta_j) - f_0 \\ &\vdots \end{aligned} \tag{40}$$

We note that equation (40) requires the evaluation of expectation terms $\mathbb{E}[\Theta_r|\theta_i]$, where $r = 1, \ldots, p$. To analytically evaluate these terms, we partition Θ and $\mathbf{V}$ as follows

$$\boldsymbol{\Theta} = [\boldsymbol{\Theta}_1\boldsymbol{\Theta}_2]^T, \ \mathbf{V} = \begin{bmatrix} \mathbf{V}_{11} & \mathbf{V}_{12} \\ \mathbf{V}_{21} & \mathbf{V}_{22} \end{bmatrix}$$

where $\boldsymbol{\Theta}_1$ is $r \times 1$, $\boldsymbol{\Theta}_2$ is $(p-r) \times 1$, and the components of $\mathbf{V}$ have dimensions

$$\begin{bmatrix} r \times r & r \times (p-r) \\ (p-r) \times r & (p-r) \times (p-r) \end{bmatrix}$$

As detailed by Eaton (1983), the expected value is

$$\mathbb{E}[\boldsymbol{\Theta}_1|\boldsymbol{\theta}_2] = \boldsymbol{\mu}_1 + \mathbf{V}_{12}\mathbf{V}_{22}^{-1}(\boldsymbol{\theta}_2 - \boldsymbol{\mu}_2) \tag{41}$$

We now apply these results to relation (39). We denote the entries in the covariance matrix by

$$\mathbf{V} = \begin{pmatrix} \sigma_1^2 & \rho_{12} & \cdots & \rho_{1p} \\ \rho_{21} & \sigma_2^2 & & \\ \vdots & & \ddots & \\ \rho_{p1} & & & \sigma_p^2 \end{pmatrix}$$

We can then express the component functions (40) as

$$\begin{aligned} f_0 &= a_1\mu_1 + \cdots + a_p\mu_p \\ f_i(\theta_i) &= a_i\theta_i + \sum_{\substack{j=1 \\ j\neq i}}^{p} a_j\left(\mu_j + \rho_{\sigma_i\sigma_j}\frac{\sigma_j}{\sigma_i}(\theta_i - \mu_i)\right) \\ &\quad - f_0, \quad (i = 1, \ldots, p) \\ f_{ij}(\theta_i,\theta_j) &= a_i\theta_i + a_j\theta_j \\ &\quad + \sum_{\substack{k=1 \\ k\neq i,j}}^{p} a_k\left(\mu_k + [\rho_{ki}\ \rho_{kj}]\begin{bmatrix} \sigma_i^2 & \rho_{ij} \\ \rho_{ji} & \sigma_j^2 \end{bmatrix}^{-1}\begin{bmatrix} \theta_i - \mu_i \\ \theta_j - \mu_j \end{bmatrix}\right) \\ &\quad - f_i - f_j - f_0 \\ &\vdots \\ f_{1,\ldots,p}(\theta_1, \ldots, \theta_p) &= f(\theta) - \cdots - \sum_{1 \le i<j<k<\ell \le p} f_{ijk\ell} \\ &\quad - \sum_{1 \le i<j<k \le p} f_{ijk} - \sum_{1 \le i<j \le p} f_{ij} - \sum_{i=1}^{p} f_i - f_0 \end{aligned} \tag{42}$$

Here, $\rho_{\sigma_i\sigma_j} = \rho_{ij}/(\sigma_i\sigma_j)$ is the Pearson correlation, ρ_{ij} the covariance between θ_i and θ_j, and σ_i^2 is the variance for θ_i. We present results, obtained when employing this methodology for the monodomain model, in the "Results" section.

Spline basis functions expansion

The analytical solution technique, detailed in the previous section, is only applicable for linearly parameterized problems. Here, we discuss a general solution technique for nonlinearly parameterized problems $Y = f(\theta)$. This technique is based on the work in Li et al. (2010) and utilizes cubic B-splines (Hastie et al., 2009; Prenter, 1989), $B_k(\theta)$, $k = -1, \ldots, m+1$, to approximate the terms in the HDMR representation for $Y = f(\theta)$. Specifically, the component terms in equation (23) are represented as

$$\begin{aligned} f_i(\theta_i) &\approx \sum_{r=-1}^{m+1} \alpha_r^i B_r(\theta_i) \\ f_{ij}(\theta_i,\theta_j) &\approx \sum_{u=-1}^{m+1}\sum_{q=-1}^{m+1} \beta_{uq}^{ij} B_u(\theta_i) B_q(\theta_j) \\ f_{ijk}(\theta_i,\theta_j,\theta_k) &\approx \sum_{u=-1}^{m+1}\sum_{q=-1}^{m+1}\sum_{v=-1}^{m+1} \gamma_{uqv}^{ijk} B_u(\theta_i) B_q(\theta_j) B_v(\theta_k) \end{aligned} \tag{43}$$

where coefficients $\alpha_r^i, \beta_{uq}^{ij}$, and γ_{uqv}^{ijk} are to be determined via least squares regression. The first-, second-, and third-order component functions are approximated by

$$\begin{aligned} f_i(\theta_i^s) &\approx Y^s - f_0 \\ f_{ij}(\theta_i^s,\theta_j^s) &\approx Y^s - f_0 - f_i(\theta_i^s) - f_j(\theta_j^s) \\ f_{ijk}(\theta_i^s,\theta_j^s,\theta_k^s) &\approx Y^s - f_0 - f_i(\theta_i^s) - f_j(\theta_j^s) \\ &\quad - f_k(\theta_k^s) - f_{ij}(\theta_i^s,\theta_j^s) - f_{ik}(\theta_i^s,\theta_k^s) - f_{jk}(\theta_j^s,\theta_k^s) \end{aligned} \tag{44}$$

Here, $Y^s = f(\theta^s)$ is employed as an unbiased estimator for $\mathbb{E}[Y|\theta_{r_n}^s]$ and θ^s represents realizations from the underlying distribution for θ. Substituting the expressions (43) into (44) yields

$$\begin{aligned} &\sum_{r=-1}^{m+1} \alpha_r^i B_r(\theta_i^s) \approx Y^s - f_0 \\ &\sum_{u=-1}^{m+1}\sum_{q=-1}^{m+1} \beta_{uq}^{ij} B_u(\theta_i^s) B_q(\theta_j^s) \\ &\approx Y^s - f_0 - f_i(\theta_i^s) - f_j(\theta_j^s) \\ &\sum_{u=-1}^{m+1}\sum_{q=-1}^{m+1}\sum_{v=-1}^{m+1} \gamma_{uqv}^{ijk} B_u(\theta_i^s) B_q(\theta_j^s) B_v(\theta_k^s) \\ &\approx Y^s - f_0 - f_i(\theta_i^s) - f_j(\theta_j^s) - f_k(\theta_k^s) \\ &\quad - f_{ij}(\theta_i^s,\theta_j^s) - f_{ik}(\theta_i^s,\theta_k^s) - f_{jk}(\theta_j^s,\theta_k^s) \end{aligned} \tag{45}$$

To determine the coefficients $\alpha^i = [\alpha_{-1}^i, \ldots, \alpha_{m+1}^i]^T$, we minimize the cost functional

$$\begin{aligned} J_i(\alpha^i) &= \sum_{s=1}^{K} \left(Y^s - f_0 - f_i(\theta_i^s)\right)^2 \\ &= \sum_{s=1}^{K} \left(Y^s - f_0 - \sum_{r=-1}^{m+1} \alpha_r^i B_r(\theta_i^s)\right)^2 \\ &= \left(\mathbf{Y}^i - \mathbf{A}^{\{i\}}\alpha^i\right)^T \left(\mathbf{Y}^i - \mathbf{A}^{\{i\}}\alpha^i\right) \\ &= \left\|\mathbf{Y}^i - \mathbf{A}^{\{i\}}\alpha^i\right\|_2^2 \end{aligned} \tag{46}$$

for $i = 1, \ldots, p$. Here

$$\mathbf{A}^{\{i\}} = \begin{bmatrix} B_{-1}(\theta_i^1) & B_0(\theta_i^1) & \cdots & B_{m+1}(\theta_i^1) \\ \vdots & \vdots & & \vdots \\ B_{-1}(\theta_i^K) & B_0(\theta_i^K) & \cdots & B_{m+1}(\theta_i^K) \end{bmatrix}$$

$$\mathbf{Y}^i = \begin{bmatrix} Y^1 \\ \vdots \\ Y^K \end{bmatrix} - f_0 1$$

$1 = [1, \ldots, 1]^T$, and K is the number of samples of θ. Hence, we obtain the least squares solution

$$\alpha^{i*} = \left(\mathbf{A}^{\{i\}^T}\mathbf{A}^{\{i\}}\right)^{-1}\mathbf{A}^{\{i\}^T}\mathbf{Y}^i \tag{47}$$

to the sum of squares cost function (46). It follows that the first-order component functions satisfy $\mathbf{Y}^1 = \cdots = \mathbf{Y}^p$.

Similarly, for

$$\beta^{ij} = [\beta_{-1,-1}^{ij}, \ldots, \beta_{m+1,-1}^{ij}, \beta_{-1,0}^{ij}, \ldots, \beta_{uq}^{ij}, \ldots, \beta_{m+1,m+1}^{ij}]^T$$

and

$$\gamma^{ijk} = [\gamma_{-1,-1,-1}^{ijk}, \ldots, \gamma_{uqv}^{ijk}, \ldots, \gamma_{m+1,m+1,m+1}^{ijk}]^T$$

we minimize the cost functions

$$\begin{aligned} J_{ij}(\beta^{ij}) &= \left\|\mathbf{Y}^{ij} - \mathbf{A}^{\{ij\}}\beta^{ij}\right\|_2^2 \\ J_{ijk}(\gamma^{ijk}) &= \left\|\mathbf{Y}^{ijk} - \mathbf{A}^{\{ijk\}}\gamma^{ijk}\right\|_2^2 \end{aligned}$$

In the "Results" section, we compare the results of using the analytical method of computing the component functions presented the previous section with the method presented in this section for the monodomain model.

Fisher information matrix

The Fisher information matrix contains local sensitivity information that can be exploited to determine

unidentifiable or noninfluential parameters. To motivate, we consider a scalar-valued response

$$Y = f(P^n; \theta), \quad n = 1, \ldots, N$$

where P^n are prescribed polarization values. For example, this could be the polarization energy

$$Y = u_P\left(P_2^n, P_3^n; \theta_P\right)$$

defined in equation (6) and employed in equation (16) when constructing a pseudoresponse. We let Y_n denote data at the same N polarization values.

Minimization of the functional

$$J(\theta) = \frac{1}{N}\sum_{n=1}^{N}\left[Y_n - f(P^n; \theta)\right]^2$$

yields an optimal parameter vector θ^*. As detailed in the "Introduction,"θ is locally identifiable at θ^* if this minimum is uniquely determined by data.

To relate to local sensitivity, we consider the multivariate Taylor expansion

$$f(P^n; \theta) \approx f(P^n; \theta^*) + \nabla_\theta f(P^n; \theta^*) \cdot \Delta\theta$$

where

$$\nabla_\theta f(P^n; \theta^*) = \left[\frac{\partial f}{\partial \theta_1}(P^n; \theta^*), \ldots, \frac{\partial f}{\partial \theta_p}(P^n; \theta^*)\right]^T \quad (48)$$

and $\Delta\theta = \theta - \theta^*$. Based on the assumption that $Y_n \approx f(P^n; \theta^*)$ at the minimum θ^*, the cost functional can be approximated by

$$J(\theta) \approx \frac{1}{N}\sum_{n=1}^{N}\left[\nabla_\theta f(P^n; \theta^*) \cdot \Delta\theta\right]^2$$

If we define the $N \times p$ sensitivity matrix S by

$$S = \begin{bmatrix} \frac{\partial f}{\partial \theta_1}\left(P^1; \theta^*\right) & \cdots & \frac{\partial f}{\partial \theta_p}\left(P^1; \theta^*\right) \\ \vdots & & \vdots \\ \frac{\partial f}{\partial \theta_1}\left(P^N; \theta^*\right) & \cdots & \frac{\partial f}{\partial \theta_p}\left(P^N; \theta^*\right) \end{bmatrix} \quad (49)$$

we can then approximate the cost functional by

$$J(\theta) \approx \frac{1}{N}(S\Delta\theta)^T(S\Delta\theta)$$

or, equivalently, $J(\theta^* + \Delta\theta) \approx (1/N)\Delta\theta^T S^T S \Delta\theta$. If we take $\Delta\theta$ to be an eigenvector of $S^T S$, so that $S^T S \Delta\theta = \lambda \Delta\theta$, then

$$J(\theta^* + \Delta\theta) \approx \frac{1}{N}\lambda \parallel \Delta\theta \parallel_2^2$$

We note that if $\lambda \approx 0$, the cost functional perturbations $J(\theta^* + \Delta\theta)$ are also approximately 0 and hence the corresponding parameters are locally unidentifiable. This forms the basis for the algorithms in the works by Brun et al. (2002), Burth et al. (1999), Contron-Arias et al. (2009) and Quaiser and Monnigmann (2009). We employ Algorithm 3.2 from the work by Quaiser and Monnigmann (2009).

Results

In the next section, we illustrate the analytical and numerical techniques from the last section for quantifying the global sensitivity of the parameters (equation (14)) in the linearly parameterized models $Y_P(\theta_P)$ (equation (16)), $Y_{\sigma_{ns}}(\theta_{\sigma_{ns}})$ (equation (17)), and $Y_{\sigma_s}(\theta_{\sigma_s})$ (equation (18)) for correlated parameters. We illustrate in section "Global sensitivity analysis: assumption of independent parameters," the discrepancies that arise if one performs global sensitivity analysis based on the incorrect assumption that parameters are independent and uniformly distributed. In the final section, we will use local sensitivity analysis, based on the Fisher information matrix discussed in "Fisher information matrix" to isolate unidentifiable parameters.

Global sensitivity analysis

Analytical determination of component functions. To construct the component functions (equation (23)), we must first specify a prior distribution for the parameters. We obtained nominal values for θ_P, $\theta_{\sigma_{ns}}$, and θ_{σ_s} via Bayesian inference by calibrating using synthetic

Algorithm 3.2: Parameter subset selection algorithm to determine locally unidentifiable parameters (Quaiser and Monnigmann, 2009).

(0) Set $\eta = p$, where p is the number of parameters in the model, and construct the sensitivity matrix S following relation (49).

We note that the variable η changes with the iterations of the algorithm.

(1) Compute the matrix $S^T S$ and its eigenvalues and order their magnitudes as $|\lambda_1| \leq |\lambda_2| \leq \cdots \leq |\lambda_\eta|$.
(2) If $|\lambda_1| > \epsilon$, where ϵ is some prescribed threshold value, stop. We take all the parameters to be identifiable.
(3) If $|\lambda_1| < \epsilon$, then one of the parameters is not identifiable. Proceed as follows.
(4) Identify the component with the largest magnitude in the eigenvector $\Delta\theta_1$ associated with λ_1. This component corresponds to the least identifiable parameter.
(5) Remove the column in S corresponding to the component identified in Step 4, set $\eta = \eta - 1$ and repeat Step 1.

Table 1. Mean parameter values obtained through Bayesian inference in the work Miles et al. (2018).

Parameter	α_1	α_{11}	α_{12}	α_{111}	α_{112}
Units	MV m/C	MV m^5/C^3	MV m^5/C^3	MV m^9/C^5	MV m^9/C^5
Mean value ($\boldsymbol{\mu}_u$)	−389.4	761.3	414.1	61.46	−740.8
Standard deviation	10.49	30.01	241.6	19.98	499.4
Parameter	q_{11}	q_{12}	σ^R_{11}	σ^R_{22}	σ^R_{33}
Units	GV m/C	GV m/C	GPa	GPa	GPa
Mean value ($\boldsymbol{\mu}_{ns}$)	19.2	3.14	−3.98	−4.00	−3.41
Standard deviation	0.258	0.182	0.103	0.101	0.118
Parameter	q_{44}	σ^R_{23}			
Units	GV m/C	GPa			
Mean value ($\boldsymbol{\mu}_s$)	1.40	−8.16e−4			
Standard deviation	0.019	3.32e−3			

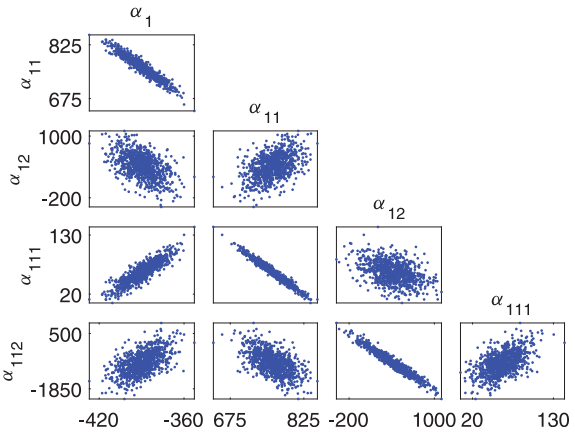

Figure 4. Pairwise correlation among the Landau energy parameters $\theta_P = [\alpha_1, \alpha_{11}, \alpha_{12}, \alpha_{111}, \alpha_{112}]$.

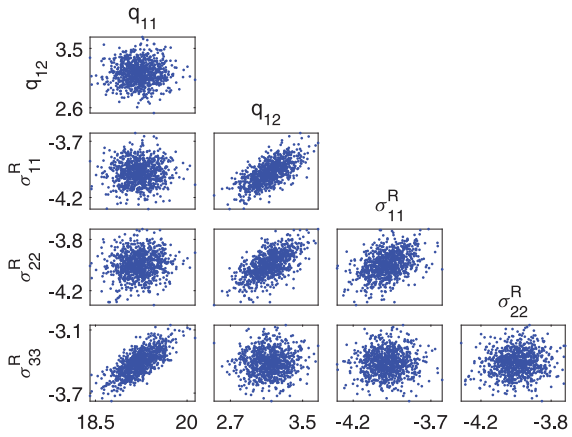

Figure 5. Pairwise correlation among the normal stress parameters $\theta_{\sigma_{ns}} = [q_{11}, q_{12}, \sigma^R_{11}, \sigma^R_{22}, \sigma^R_{33}]$.

data computed via DFT simulations (Oates, 2014). As detailed in Miles et al. (2018), we use the Delayed Rejection Adaptive Metropolis (DRAM) algorithm (Haario et al., 2006; Smith, 2014) to perform the Bayesian analysis. We summarize the nominal values in Table 1. We plot the resulting joint pairwise correlation plots for θ_P, $\theta_{\sigma_{ns}}$, θ_{σ_s} in Figures 4 to 6.

We also obtained the covariance matrices

$$\mathbf{V}_P = \begin{pmatrix} 105.65 & -287.05 & -1.3069\text{e}+3 & 177.38 & 2.9320\text{e}+3 \\ -287.05 & 854.09 & 3.4852\text{e}+3 & -556.86 & -8.4947\text{e}+3 \\ 1.3069\text{e}+3 & 3.4852\text{e}+3 & 5.3605\text{e}+4 & -2.0918\text{e}+3 & -1.0741\text{e}+5 \\ 177.38 & -556.86 & -2.0918\text{e}+3 & 376.36 & 5.3725\text{e}+3 \\ 2.9320\text{e}+3 & -8.4947\text{e}+3 & -1.0741\text{e}+5 & 5.3725\text{e}+3 & 2.2692\text{e}+5 \end{pmatrix}$$

$$\mathbf{V}_{\sigma_{ns}} = \begin{pmatrix} 0.0605 & 0.0014 & 0.0012 & 0.0021 & 0.0208 \\ 0.0014 & 0.0314 & 0.0115 & 0.0106 & 8.8239\text{e}-4 \\ 0.0012 & 0.0115 & 0.0097 & 0.0037 & 6.3619\text{e}-4 \\ 0.0021 & 0.0106 & 0.0037 & 0.0093 & 8.4661\text{e}-4 \\ 0.0208 & 8.8239\text{e}-4 & 6.3619\text{e}-4 & 8.4661\text{e}-4 & 0.0126 \end{pmatrix} \tag{50}$$

$$\mathbf{V}_{\sigma_s} = \begin{pmatrix} 3.4801\text{e}-4 & 3.6383\text{e}-5 \\ 3.6383\text{e}-5 & 1.1141\text{e}-5 \end{pmatrix}$$

via Bayesian inference.

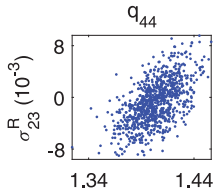

Figure 6. Pairwise correlation among the shear stress parameters $\theta_{\sigma_s} = [q_{44}, \sigma^R_{23}]$.

To construct distributions required to analytically construct or numerically approximate the component functions $f_0, f_i, \ldots$ and Sobol' indices, we take

$$\Theta_P \sim \mathcal{N}(\boldsymbol{\mu}_P, \mathbf{V}_P),\ \Theta_{\sigma_{ns}} \sim \mathcal{N}(\boldsymbol{\mu}_{ns}, \mathbf{V}_{\sigma_{ns}})$$
$$\Theta_{\sigma_s} \sim \mathcal{N}(\boldsymbol{\mu}_s, \mathbf{V}_{\sigma_s})$$

where $\boldsymbol{\mu}_P$, $\boldsymbol{\mu}_{ns}$, and $\boldsymbol{\mu}_s$ are the nominal values from Table 1 and the covariance matrices are defined in equation (50). We note that this is an approximation to obtain parametric distributions from the non-parametric posterior distributions created through Bayesian analysis. As an alternative to Bayesian inference, one could use asymptotic ordinary least squares (OLS) techniques or experimental data to obtain nominal values and covariance matrices.

Numerical determination of component functions. Using the numerical method detailed in the section on "Spline basis functions expansion," we first solve the least squares problem (47) to compute the coefficients α^{i*} used in equation (43) to approximate $f_i(\theta_i)$. We then compute coefficients β^{ij} and γ^{ijk} to compute second- and third-order effects $f_{ij}(\theta_i, \theta_j)$ and $f_{ijk}(\theta_i, \theta_j, \theta_k)$. The samples for the procedure in this section are also taken from the distributions $\mathcal{N}(\boldsymbol{\mu}_P, \mathbf{V}_P)$, $\mathcal{N}(\boldsymbol{\mu}_{ns}, \mathbf{V}_{\sigma_{ns}})$, and $\mathcal{N}(\boldsymbol{\mu}_s, \mathbf{V}_{\sigma_s})$.

Sobol' sensitivity indices. The first-order Sobol' indices S_i, $i = 1, \ldots, p$, quantify the fraction of uncertainty in the response that can be attributed to θ_i, whereas higher-order sensitivity indices S_{ij}, $i<j$, S_{ijk}, $i<j<k$, ..., quantify the uncertainty due to interactions and correlations that can be attributed to the parameters. The total indices S_{T_i} quantify the total fraction of uncertainty that can be attributed to θ_i and its higher-order structural interactions and correlation contributions with other parameters. Hence, S_{T_i} provides a more comprehensive measure of global parameter sensitivity.

Here, we construct the sensitivity indices for each of the component functions f_{r_n}. We determine the component functions f_{r_n} using the analytical and numerical methods of the previous section. We employ the Monte Carlo approximations

$$\begin{aligned} S_{r_n} &= \frac{\mathrm{cov}[f_{r_n}, Y]}{\mathrm{var}[Y]} \approx \frac{\sum_{s=1}^{K} f_{r_n}\left(\theta^s_{r_n}\right)[f(\theta^s) - f_0]}{\sum_{s=1}^{K}[f(\theta^s) - f_0]^2} \\ S^s_{r_n} &= \frac{\mathrm{var}[f_{r_n}]}{\mathrm{var}[Y]} \approx \frac{\sum_{s=1}^{K} {f_{r_n}}^2(\theta^s)}{\sum_{s=1}^{K}[f(\theta^s) - f_0]^2} \\ S^c_{r_n} &= S_{r_n} - S^s_{r_n} \end{aligned} \tag{51}$$

where f_0 is approximated by the sample mean

$$f_0 \approx \frac{\sum_{s=1}^{K} f(\theta^s)}{K}$$

Using these approximations, we obtain the results in Table 2 for θ_P, Table 3 for $\theta_{\sigma_{ns}}$, and Table 4 for θ_{σ_s}. Note that we used $K = 10,000$ samples to compute the sensitivity indices with Monte Carlo quadrature. For the pairs of parameters that are most correlated, and whose individual parameters are most influential in θ_P, second-order sensitivity indices are significant. We make a similar observation for the normal stress parameters $\theta_{\sigma_{ns}}$ as illustrated in Table 3. We find that due to the contribution effects corresponding to parameter correlation, no parameter is noninfluential as exhibited by the total sensitivity indices for θ_P, $\theta_{\sigma_{ns}}$, and θ_{σ_s}.

We plot in Figure 7 the first-order and total sensitivity indices S_i and S_{T_i} for the Landau parameters θ_P. In Figures 8 and 9, we plot the sensitivity indices S_i and S_{T_i} for normal and shear stress parameters $\theta_{\sigma_{ns}}$ and θ_{σ_s}, respectively.

We note that the magnitudes for the first-order sensitivity indices S_3 and S_5 are relatively small for the parameters α_{12} and α_{112}. However, correlative contributions present in the higher-order sensitivity indices and compiled in Table 2 have a non-negligible effect on the total sensitivity indices S_{T_3} and S_{T_5}. This implies that the parameters $\theta_3 = \alpha_{12}$ and $\theta_5 = \alpha_{112}$ are still influential.

We make a similar observation regarding the electrostrictive coefficients q_{11} and q_{12}. Although, first-order contributions are negligible, second- and third-order interactions, as observed in Table 3, yield greater total sensitivity indices, making the coefficients more influential. We observe from Table 4 that while the first-order contribution is negligible for q_{44}, the second-order sensitivity index for q_{44} and σ^R_{23} is significant in the case of the shear stress. This yields a considerable contribution to the total sensitivity indices S_{T_i}, making both parameters q_{44} and σ^R_{23} influential.

To illustrate relative effects of first-order and higher-order effects, we plot in Figures 10 to 12, the component functions for θ_P, $\theta_{\sigma_{ns}}$, and θ_{σ_s}. We note that the higher-order component functions are significant in all three cases.

Since the parameters θ_P are highly correlated, as illustrated by the covariance matrix (equation (50)) and the pairwise plots of Figure 4, we conclude that all the component functions of equation (16) are significant.

Table 2. Sensitivity indices for total contributions S_{r_n} constructed using the component functions f_{r_n} for the Landau energy parameters θ_P.

	S_1	S_2	S_3	S_4	S_5					
A. 1st order	0.281	0.133	0.006	0.088	0.009					
N. 1st order	0.274	0.127	0.005	0.082	0.008					
	S_{12}	S_{13}	S_{14}	S_{15}	S_{23}	S_{24}	S_{25}	S_{34}	S_{35}	S_{45}
A. 2nd order	0.100	0.062	0.060	0.067	0.012	0.021	0.016	−3.75e−4	0.002	−0.001
N. 2nd order	0.109	0.065	0.068	0.072	0.014	0.029	0.019	0.002	0.004	0.002
	S_{123}	S_{124}	S_{125}	S_{134}	S_{135}	S_{145}	S_{234}	S_{235}	S_{245}	S_{345}
A. 3rd order	−0.002	0.049	−0.052	0.013	−0.069	−0.024	0.032	−0.011	0.015	0.001
N. 3rd order	4.20e−4	0.036	−0.052	0.016	−0.068	−0.023	0.036	−0.009	0.018	0.003
	S_{1234}	S_{1235}	S_{1245}	S_{1345}	S_{2345}					
A. 4th order	−0.070	0.202	−0.011	0.088	−0.025					
N. 4th order	−0.073	0.195	−0.011	0.092	−0.011					
	S_{12345}									
A. 5th order	0.009									
N. 5th order	−0.027									
	S_{T_1}	S_{T_2}	S_{T_3}	S_{T_4}	S_{T_5}					
A. Total index	0.703	0.418	0.249	0.244	0.217					
N. Total index	0.672	0.400	0.242	0.238	0.211					

The A's and N's represent sensitivity indices derived from the analytical and numerical determination of the component functions, respectively. The indices correspond to the order specified by $\theta_P = [\alpha_1, \alpha_{11}, \alpha_{12}, \alpha_{111}, \alpha_{112}]$. The shaded cells designate significant indices.

Table 3. Sensitivity indices for total contributions S_{r_n} constructed using the component functions f_{r_n} for the normal stress parameters $\theta_{\sigma_{ns}}$.

	S_1	S_2	S_3	S_4	S_5					
A. 1st order	5.79e−4	0.001	0.158	0.176	0.164					
N. 1st order	5.46e−4	0.001	0.156	0.179	0.162					
	S_{12}	S_{13}	S_{14}	S_{15}	S_{23}	S_{24}	S_{25}	S_{34}	S_{35}	S_{45}
A. 2nd order	5.74e−5	−5.79e−4	−4.50e−4	0.180	0.157	0.141	0.002	−0.093	−0.018	−0.025
N. 2nd order	7.42e−4	2.09e−4	9.70e−4	0.183	0.156	0.141	0.002	−0.092	−0.015	−0.023
	S_{123}	S_{124}	S_{125}	S_{134}	S_{135}	S_{145}	S_{234}	S_{235}	S_{245}	S_{345}
A. 3rd order	−5.73e−5	3.35e−4	1.47e−5	6.99e−4	0.003	0.016	0.120	0.001	−0.003	0.012
N. 3rd order	0.003	0.003	0.003	0.005	0.005	0.017	0.119	0.001	−0.003	0.014
	S_{1234}	S_{1235}	S_{1245}	S_{1345}	S_{2345}					
A. 4th order	0.002	0.003	0.013	−0.005	−0.012					
N. 4th order	0.006	0.009	0.016	0.005	−0.011					
	S_{12345}									
A. 5th order	0.005									
N. 5th order	−0.045									
	S_{T_1}	S_{T_2}	S_{T_3}	S_{T_4}	S_{T_5}					
A. Total index	0.217	0.431	0.334	0.348	0.336					
N. Total index	0.211	0.403	0.316	0.332	0.320					

The indices correspond to the order specified by $\theta_{\sigma_{ns}} = [q_{11}, q_{12}, \sigma^R_{11}, \sigma^R_{22}, \sigma^R_{33}]$. The shaded cells correspond to significant indices.

Table 4. Sensitivity indices for total contributions S_{r_n} constructed using the component functions f_{r_n} for the shear stress parameters $\theta_{\sigma_{ns}}$.

	S_1	S_2	S_{12}	S_{T_1}	S_{T_2}
Sensitivity	6.812e−5	0.651	0.349	0.349	1.000
Numerical	5.347e−5	0.650	0.350	0.350	1.000

The indices correspond to the order specified by $\theta_{\sigma_{ns}} = [q_{11}, q_{12}, \sigma^R_{11}, \sigma^R_{22}, \sigma^R_{33}]$. The shaded cells designate significant indices.

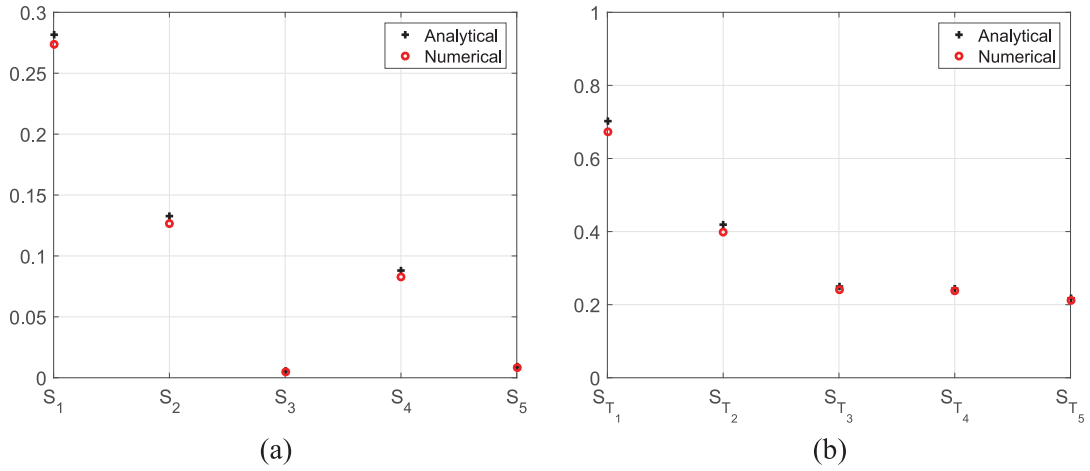

Figure 7. Comparison of analytical and numerical methods obtain (a) first-order and (b) total sensitivity indices for equation (16).

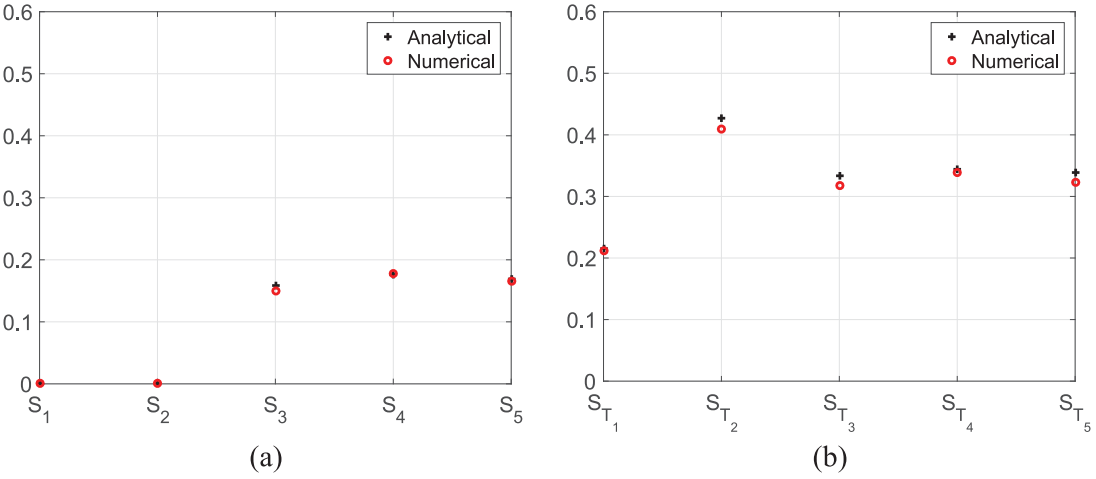

Figure 8. Comparison of analytical and numerical methods to obtain (a) first-order and (b) total sensitivity indices for equation (17).

For the normal stress electrostrictive parameters $\theta_{\sigma_{ns}}$, it is shown that higher-order component functions are significant for the sets of most correlated parameters. Finally, for the shear stress parameters, the second-order component function is again significant due to the correlation between q_{44} and σ^R_{23}.

Global sensitivity analysis: assumption of independent parameters

The pairwise plots in Figures 4 to 6, obtained through Bayesian inference, demonstrate that the parameters are highly correlated, thus requiring the general sensitivity analysis. The results in the section on "Global sensitivity analysis" demonstrate that due to this correlation, high-order indices can be significant when first-order interactions are negligible.

As noted in the "Introduction," however, the nature of parameter correlation is rarely known a priori thus motivating global sensitivity analysis based on the assumption of mutually independent, uniformly distributed parameters. As detailed in the section on "Sobol' indices for independent parameters with uniform

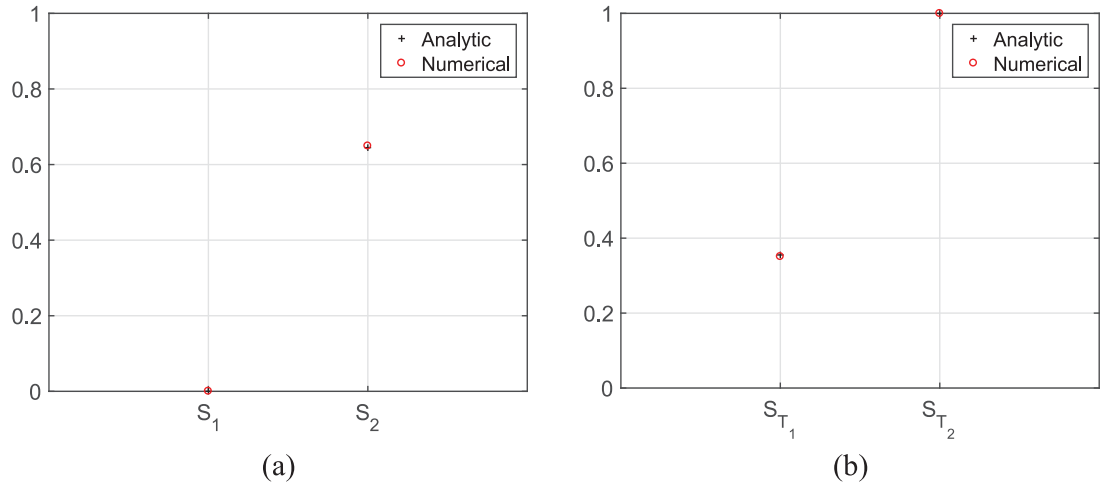

Figure 9. Comparison of analytical and numerical methods to obtain (a) first-order and (b) total sensitivity indices for equation (18).

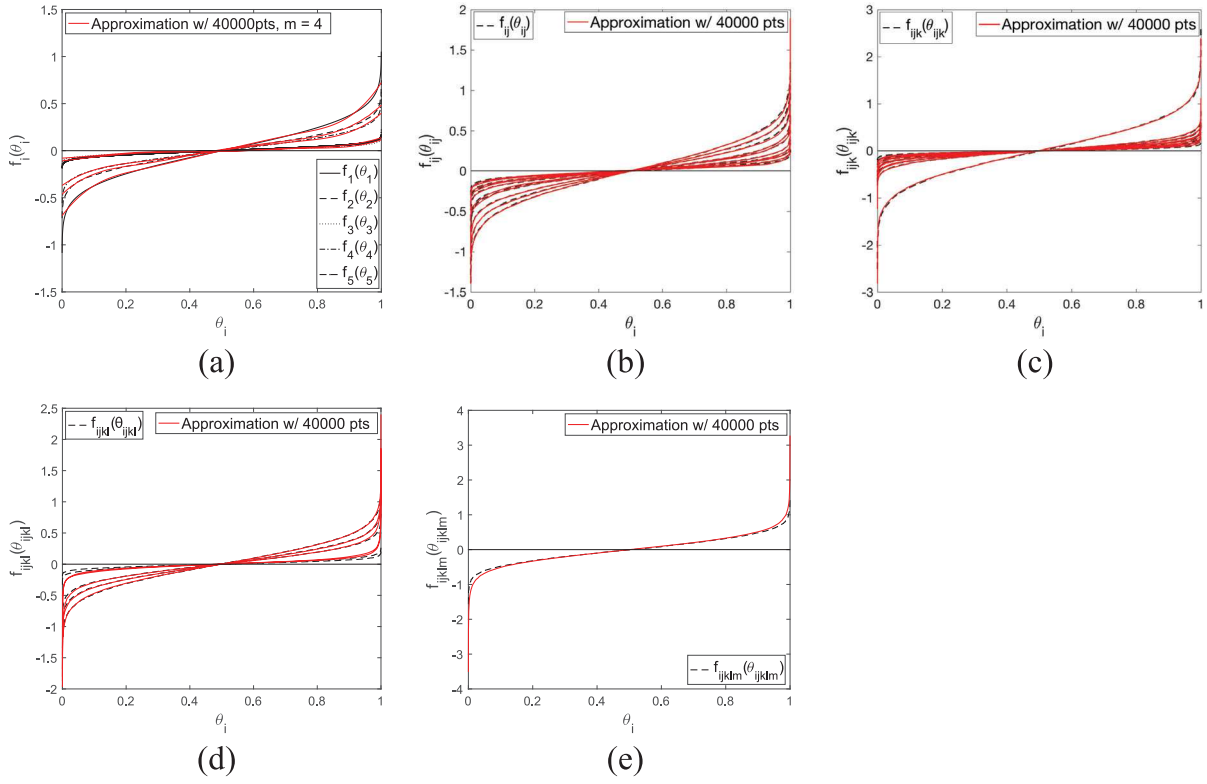

Figure 10. (a) First-, (b) second-, (c) third-, (d) fourth-, and (e) fifth-order component functions constructed using the analytical method (– –) and the numerical method (—) for θ_p in equation (16) with m = 4 subintervals for the cubic B-spline basis functions.

densities," this vastly simplifies the computation of Sobol' indices. We will demonstrate here, however, that this also yields incorrect and highly misleading measures of parameter influence and ranking when parameters are correlated.

We consider the parameters to be independent and uniformly distributed

$$\Theta_i \sim \mathcal{U}\left(\theta_i^{nom} - 0.25\left|\theta_i^{nom}\right|, \theta_i^{nom} + 0.25\left|\theta_i^{nom}\right|\right)$$

where $|\theta_i^{nom}|$ are the absolute values of nominal values compiled in Table 1 for θ_P in equation (12) and θ_σ in equation (13). Perturbations on the order of 0.25 are commonly employed to provide broad sampling without significantly changing the model behavior. To avoid scaling issues, we mapped these intervals to

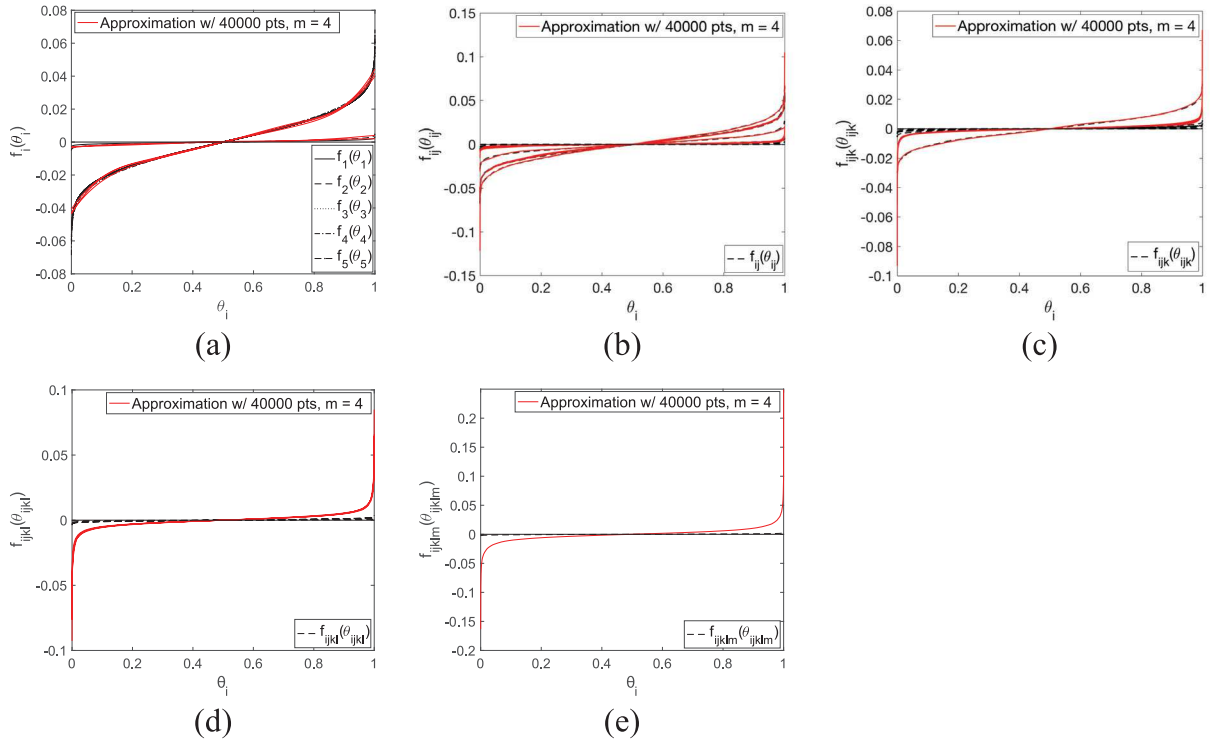

Figure 11. (a) First-, (b) second-, (c) third-, (d) fourth-, and (e) fifth-order component functions constructed using the analytical method (– –) and numerical method (—) for θ_{σ_s} in equation (17) with $m = 4$ subintervals.

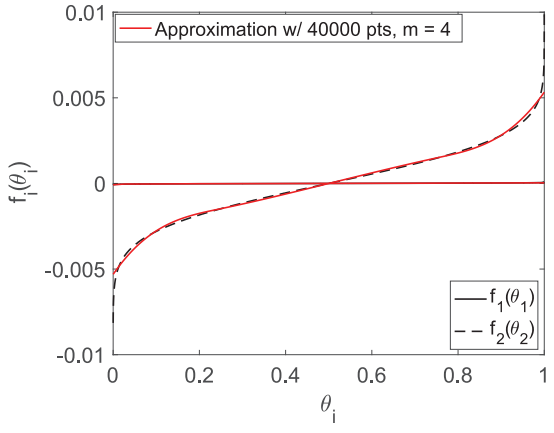

Figure 12. First-order component functions constructed using the analytical method (– –) and numerical method (—) for θ_{σ_s} in equation (18) with $m = 4$ subintervals.

$[0, 1]$ before employing Algorithm 3.1 to approximate first- and second-order Sobol' indices. We employed $M = 10,000$ samples when constructing Y_A, Y_B, and Y_{C_i}, $i = 1, \ldots, p$ for the polarization energy pseudoresponse (equation (16)), the normal stress pseudoresponse (equation (17)), and the shear stress pseudoresponse (equation (18)).

We summarize in Table 5 the first-order and total Sobol' indices for the three parameter sets. We note that the indices S_i and S_{T_i} imply that α_1 and α_{11} are most influential and they reflect the property (33), which states that the first- and second-order indices sum to unity. Likewise, the indices for the normal stress components imply that q_{12}, σ^R_{11}, and σ^R_{33} are most influential and satisfy equation (33). The indices for the shear stress parameters show that σ^R_{23} is most influential, also satisfying equation (33).

These results indicate that the Landau energy parameters α_{12}, α_{111}, and α_{112}, normal stress parameters

Table 5. Sobol' indices S_i, S_{T_i} for responses $Y_P(\theta_P)$, $Y_{\sigma_{ns}}(\theta_{\sigma_{ns}})$, and $Y_{\sigma_s}(\theta_{\sigma_s})$, constructed using Algorithm 3.1.

	α_1	α_{11}	α_{12}	α_{111}	α_{112}	q_{11}	q_{12}	σ^R_{11}	σ^R_{22}	σ^R_{33}	q_{44}	σ^R_{23}
S_i	0.40	0.60	4.35e−5	1.12e−3	1.49e−4	2.26e−2	0.29	0.16	3.25e−3	0.51	3.84e−3	0.99
S_{T_i}	0.40	0.59	1.97e−4	1.89e−3	1.44e−4	2.13e−2	0.29	0.16	3.96e−3	0.52	2.95e−3	1.00

The shaded columns correspond to significant indices.

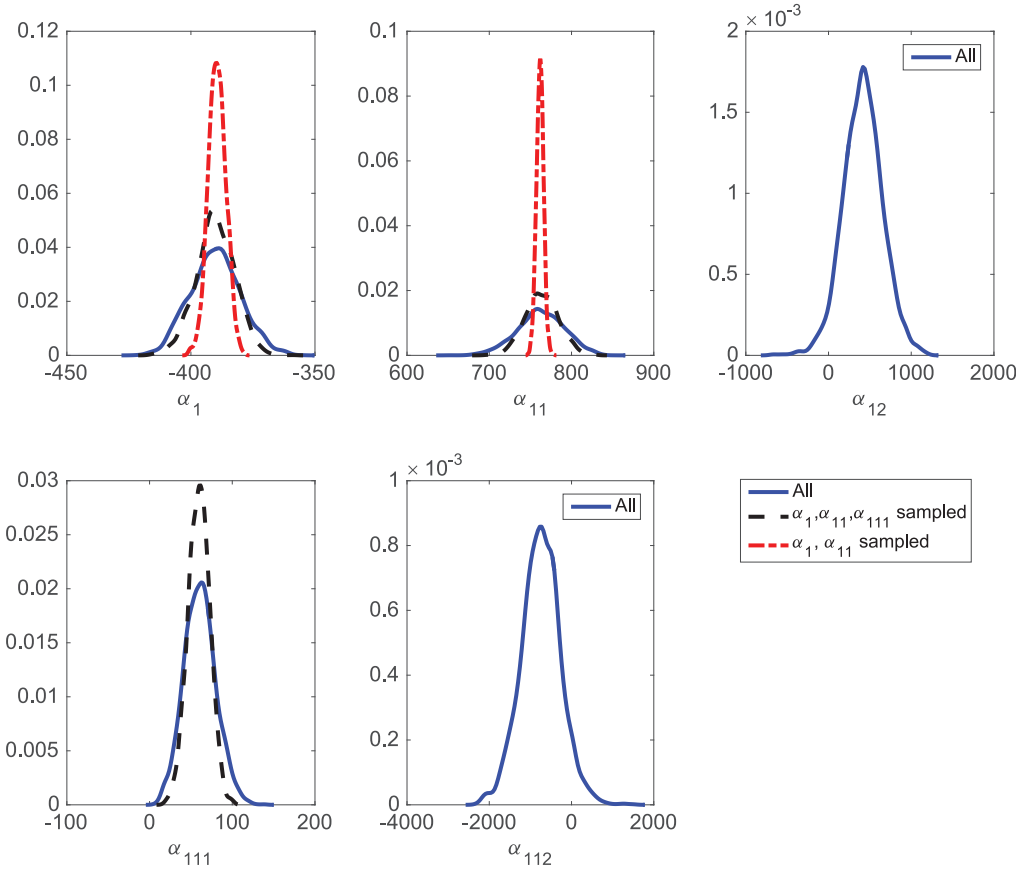

Figure 13. Posterior densities obtained via Bayesian calibration of $Y_p(\theta_P)$ in equation (16) when (1) sampling all the parameters, (2) sampling $\alpha_1, \alpha_{11}, \alpha_{111}$ with $\alpha_{12}, \alpha_{112}$ fixed, and (3) sampling α_1, α_{11} with $\alpha_{111}, \alpha_{12}, \alpha_{12}$ fixed.

q_{11}, q_{44}, and σ_{22}^R, and shear stress parameter q_{44} are not influential. Based on this result, the parameters are not influential and therefore minimal uncertainty in the response can be attributed to uncertainty in the parameters. Furthermore, these parameters could then be fixed at nominal values for Bayesian model calibration. Because the fixed parameters are not influential, we would expect negligible changes in the uncertainty quantification of the influential parameters before and after the noninfluential parameters are fixed.

We then employ the DRAM algorithm (Haario et al., 2006; Smith, 2014) to perform the Bayesian analysis and obtain posterior densities for the influential parameters, when fixing noninfluential parameters dictated by the results in Table 5. The model is once again informed by synthetic data generated by DFT simulations (Oates, 2014). We consider the cases when the noninfluential parameters α_{12}, α_{111}, and α_{112} are fixed at the nominal values presented in Table 1. We obtain the posterior densities plotted in Figure 13.

We note that the posterior densities vary significantly when (1) all the parameters are sampled and (2) the parameters α_1, α_{11} are sampled with $\alpha_{111}, \alpha_{12}, \alpha_{12}$ fixed at the nominal values. These results contradict the results in Table 5 but are consistent with the results in the section on "Global sensitivity analysis," where all parameters were found to be significant. This demonstrates that global sensitivity indices based on the assumption of mutually independent, uniformly distributed, parameters can yield very misleading interpretations of parameter influence when parameters are correlated.

Local identifiability analysis based on the Fisher information matrix

Here, we employ the local identifiability analysis methodology from the section on the "Fisher information matrix" to infer any locally unidentifiable parameters and corroborate the global sensitivity analysis results for correlated parameters. Specifically, we apply Algorithm 3.2 to the Landau polarization energy u_P in equation (6), and the normal stresses σ_{11}, σ_{22}, σ_{33}, and shear stress σ_{23} in equation (11). We note again that the Landau energy parameters are

$$\theta_P = [\alpha_1, \alpha_{11}, \alpha_{12}, \alpha_{111}, \alpha_{112}]$$

whereas the normal and shear stress coefficients are, respectively

Table 6. Results from Algorithm 3.2 to determine unidentifiable parameters in θ_P (equation (12)) for the polarization energy $Y_{\sigma_{ns}}(\theta_{\sigma_{ns}})$ (equation (6)).

Iteration	$\lvert\lambda_1\rvert$	α_1	Eigenvector $\Delta\theta_1$ with associated parameters			
			α_{11}	α_{12}	α_{111}	α_{112}
	5.62e−5	1.16e−2	−3.30e−2	−4.31e−1	2.07e−2	9.01e−1

Result: All parameters θ_P are identifiable since $|\lambda_1|>\epsilon = 10^{-8}$

Table 7. Results from Algorithm 3.2 to determine unidentifiable parameters in θ_σ (equation (13)) for the normal and shear stress components θ_{ns} and θ_s (equation (11)).

Iteration	$\lvert\lambda_1\rvert$	Eigenvector $\Delta\theta_1$ with associated parameters				
		q_{11}	q_{12}	σ^R_{11}	σ^R_{22}	σ^R_{33}
1	3.67	−9.33e−1	−6.13e−2	−2.48e−2	−5.17e−2	−3.51e−1
Iteration	$\lvert\lambda_1\rvert$	q_{44}	σ^R_{23}			
1	8.99e−1	−9.94e−1	−1.07e−2			

Result: All parameters θ_σ are identifiable since $|\lambda_1|>\epsilon = 10^{-8}$

$$\theta_{\sigma_{ns}} = \left[q_{11}, q_{12}, \sigma^R_{11}, \sigma^R_{22}, \sigma^R_{33}\right],\ \theta_{\sigma_s} = \left[q_{44}, \sigma^R_{23}\right]$$

We set the threshold parameter $\epsilon = 10^{-8}$ in Algorithm 3.2. When $|\lambda_1|>\epsilon$, all remaining parameters that have not been removed, are identifiable. For the Landau energy u_P, application of the algorithm yields that all parameters are considered to be identifiable. We observe this from the first iteration of the algorithm in Table 6. These results are consistent with the global sensitivity analysis for correlated parameters, where we showed that all total Sobol' sensitivity indices S_{T_i} were significant, thus specifying that all parameters are influential. Therefore, no parameter in the model can be fixed for subsequent Bayesian inference. Similar results are observed for the parameters θ_σ (equation (13)) in the normal and shear stress components (equation (11)). We compile the first iteration of Algorithm 3.2 in Table 7. In both cases, the magnitude of the smallest eigenvalue is $|\lambda_1|>\epsilon$. Thus, we conclude that all the parameters are identifiable. This verifies our results for the global sensitivity analysis detailed early in this section, where it was shown that all parameters θ_σ (equation (13)) were influential.

Concluding remarks

The objective of this article was to investigate and quantify the influence of parameters in a quantum-informed continuum model for single-domain ferroelectric materials. Broadly, parameters are considered to be noninfluential if perturbations through the admissible parameter space are minimally reflected in responses. Noninfluential parameters are typically fixed at nominal values during model calibration, uncertainty propagation, and model-based design and control. In this investigation, we employed global and local sensitivity analysis to quantify the relative influence of five parameters in a sixth-order Landau polarization energy and seven electrostrictive energy parameters.

Since parameter distributions are not typically known a priori, it is commonly assumed that parameters are independent and uniformly distributed when performing global sensitivity analysis. However, we demonstrate using general theory for correlated parameters, with covariance structures computed using the Bayesian analysis in Part 1 (Miles et al., 2018), that the incorrect assumption of mutually independent parameters yields incorrect conclusions regarding parameter influence for correlated parameter sets.

While the methods for sensitivity analysis presented in other investigations, such as Hamby (1994), provide a technique for computing partial correlation coefficients, our study broadly accommodates the underlying correlation in the complete set of parameters. Hence, this analysis enables the comparison of individual, partial, and total effects due to the correlation structure.

Based on the general theory of global sensitivity analysis, we demonstrate that for both parameter sets, individual effects may be negligible, whereas total effects are significant due to correlation. For both parameter sets, this theory establishes that all of the parameters are influential and must be inferred during model calibration. The local sensitivity analysis, implemented using the Fisher information matrix, corroborates these conclusions. In comparison, global sensitivity analysis based on the assumption of

mutually independent parameters incorrectly specifies two influential polarization parameters and three influential electrostrictive parameters.

Generally, one would perform global sensitivity analysis *prior* to Bayesian or frequentist inference to reduce computational requirements by isolating the subset of identifiable parameters. This raises the practical question of how one determines whether parameters are correlated and what their distribution is *without* performing full Bayesian inference as we have done here for illustrative purposes.

One can determine whether parameters are correlated by computing the local sensitivity matrix S in equation (49) and matrix

$$F = S^T S$$

employed in Step 1 of Algorithm 3.2. Specifically, parameter correlation is indicated by non-negligible off-diagonal elements of F.

As we did in this analysis, one can then consider parameters to be normally distributed, $\theta \sim \mathcal{N}(\mu, V)$, where μ and V are OLS estimates for the mean and covariance matrix. As detailed in the work by Smith (2014), the OLS estimate for V is

$$V = \frac{R^T R}{n - p} F^{-1}$$

where n is the number of observations, p is the number of parameters, and

$$R = \sum_{i=1}^{n} [y_i - f_i(\theta)]^2$$

is the residual. The OLS estimate of V is typically employed to initiate the DRAM algorithm employed in Miles et al. (2018) for Bayesian inference. Hence, this analysis comprises the first step of Bayesian inference but avoids the computationally intensive sampling.

In future work, we will extend the single-domain sensitivity and uncertainty analysis to polydomain materials by incorporating the domain wall gradient energy (Cao and Cross, 1991). This includes the development and simulation of appropriate responses.

Global and local sensitivity analyses are subset selection techniques since they isolate subsets of identifiable or influential parameters. However, they do not address models of the form $y = \theta_1 + \theta_2$ involving linear combinations of parameters. A second component of future work will focus on active subspace techniques (Bang et al., 2012; Constantine, 2015) to isolate linear identifiable subspaces. As detailed in the work by Lewis et al. (2017), one can subsequently perform Bayesian inference on these subspaces to eliminate the tight priors required for unidentifiable parameters and reduce computational requirements for moderate to high-dimensional parameter spaces.

Authors' note

Paul Miles is now affiliated to Department of Mathematics, North Carolina State University, Raleigh, NC, USA.

Declaration of conflicting interests

The author(s) declared no potential conflicts of interest with respect to the research, authorship, and/or publication of this article.

Funding

The author(s) disclosed receipt of the following financial support for the research, authorship, and/or publication of this article: The research of L.L. and R.C.S. was supported in part by the NSF Grant CMMI-1306290 Collaborative Research CDS&E, whereas the research of P.M. and W.S.O. was supported in part by the NSF Grant CMMI-1306320 Collaborative Research CDS&E. The research of L.L. was supported in part by the National Science Foundation under the grant DGE-1633587.

ORCID iD

William S Oates https://orcid.org/0000-0003-4259-5180

References

Bang Y, Abdel-Khalik HS and Hite JM (2012) Hybrid reduced order modeling applied to nonlinear models. *International Journal of Numerical Methods in Engineering* 91: 929–949.

Bilgen OC, De Marqui J, Kochersberger KB, et al. (2011) Macro-fiber composite actuators for flow control of a variable camber airfoil. *Journal of Intelligent Material Systems and Structures* 22(1): 81–91.

Brun R, Kuhni M, Siegrist H, et al. (2002) Practical identifiability of ASM2d parameters: systematic selection and tuning of parameter sets. *Water Research* 36: 4113–4127.

Burth M, Verghese G and Velez-Reyes M (1999) Subset selection for improved parameter estimation in online identification of a synchronous generator. *IEEE Transactions on Power Systems* 14: 218–225.

Cao W and Cross L (1991) Theory of tetragonal twin structures in ferroelectric perovskites with a first-order phase transition. *Physical Review, B: Condensed Matter* 44(1): 5–12.

Cattafesta L and Sheplak M (2011) Actuators for active flow control. *Annual Review of Fluid Mechanics* 43: 247–272.

Chopra I and Sirohi J (2014) *Smart Structures Theory*. New York: Cambridge University Press.

Constantine PG (2015) *Active Subspaces: Emerging Ideas for Dimension Reduction in Parameter Studies*. Philadelphia, PA: SIAM.

Contron-Arias A, Banks HT, Capald A, et al. (2009) A sensitivity matrix based methodology for inverse problem formulation. *Journal of Inverse and Ill-posed Problems* 17: 545–564.

Cropp R and Braddock R (2002) The new Morris method: an efficient second-order screening method. *Reliability Engineering and System Safety* 78: 77–83.

Eaton ML (1983) *Multivariate Statistics: A Vector Space Approach*. New York: John Wiley & Sons.

Haario H, Laine M, Mira A, et al. (2006) Dram: efficient adaptive MCMC. *Statistics and Computing* 16(4): 339–354.

Hamby DM (1994) A review of techniques for parameter sensitivity analysis of environmental models, environmental monitoring and assessment. *Environmental Monitoring and Assessment* 32: 135–154.

Hastie T, Tibshirani R and Friedman J (2009) *The Elements of Statistical Learning*. New York: Springer.

Hoffman KL and Wood RJ (2011) Myriapod-like ambulation of a segmented microrobot. *Autonomous Robots* 31: 103–114.

Jaffe B, Cook WR and Jaffe H (1971) *Piezoelectric Ceramics*. New York: Academic Press.

King-Smith R and Vanderbilt D (1994) First-principles investigation of ferroelectricity in perovskite compounds. *Physical Review B: Condensed Matter* 49: 5828–5844.

Kumar V, Hays M, Fernandez E, et al. (2011) Flow sensitive actuators for micro-air vehicles. *Smart Materials and Structures* 20: 105033.

Leo DJ (2007) *Engineering Analysis of Smart Material Systems*. Hoboken, NJ: John Wiley & Sons.

Lewis AL, Smith RC and Williams BJ (2017) Bayesian model calibration on active subspaces. In: *Proceedings of the American control conference*, Seattle, WA, 24–26 May, pp. 978–971. New York: IEEE.

Li G, Rabitz H, Yelvington P, et al. (2010) Global sensitivity analysis for systems with independent and/or correlated inputs. *Journal of Physical Chemistry A* 114: 6022–6033.

Ma X and Zabaras N (2010) An adaptive high-dimensional stochastic model representation technique for the solution of stochastic partial differential equations. *Journal of Computational Physics* 229: 3884–3915.

Malvern L (1969) *Introduction to the Mechanics of a Continuous Medium*. Englewood Cliffs, NJ: Prentice-Hall, Inc.

Miles P, Leon L, Smith R, et al. (2018) Analysis of a multiaxial quantum informed ferroelectric continuum model: Part 1 – uncertainty quantification. *Journal of Intelligent Material Systems and Structures* 29(13): 2823–2839.

Morris MD (1991) Factorial sampling plans for preliminary computational experiments. *Technometrics* 33(2): 161–174.

Nuffer J and Bein T (2006) Applications of piezoelectric materials in the transportation industry. In: *Global symposium on innovative solutions for the advancement of the transport industry*, San Sebastian, Spain, 4–6 October, pp. 1–11.

Oates WS (2014) A quantum informed continuum model for ferroelectric materials. *Smart Material Structures* 23: 104009.

Park CY, Palazotto AN, Hale CS, et al. (2017) Internal longitudinal damage detection in a steel beam using lamb waves: simulation and test study. *Journal of Intelligent Material Systems and Structures* 29: 411–422.

Pérez-Arancibia NO, Ma KY, Galloway KC, et al. (2011) First controlled vertical flight of a biologically inspired microrobot. *Bioinspiration and Biomimetics* 6: 036009.

Prenter PM (1989) *Splines and Variational Methods*. New York: John Wiley & Sons.

Quaiser T and Monnigmann M (2009) Systematic identifiability testing for unambiguous mechanistic modeling—application to JAK-STAT, MAP kinase, and NF-κB signaling pathway models. *BMC Systems Biology* 3: 50.

Rabitz H and Alis OF (1999) General foundations of high-dimensional model representations. *Journal of Mathematical Chemistry* 25: 197–233.

Saltelli A (2002) Making best use of model evaluations to compute sensitivity indices. *Computer Physics Communications* 145: 280–297.

Saltelli A, Annoni P, Azzini I, et al. (2010) Variance based sensitivity analysis of model output. Design and estimator for the total sensitivity index. *Computer Physics Communications* 181(2): 259–270.

Saltelli A, Ratto M, Andres T, et al. (2008) *Global Sensitivity Analysis: The Primer*. Chichester: John Wiley & Sons.

Saltelli A, Ratto M, Tarantola S, et al. (2006) Sensitivity analysis practices: strategies for model-based inference. *Reliability Engineering and System Safety* 91: 1109–1125.

Saltelli A, Tarantola S, Campolongo F, et al. (2004) *Sensitivity Analysis in Practice*. Chichester: John Wiley & Sons.

Scott JF (2000) *Ferroelectric Memories*. Berlin: Springer.

Smith RC (2005) *Smart Material Systems: Model Development*. Philadelphia, PA: SIAM.

Smith RC (2014) *Uncertainty Quantification: Theory, Implementation and Applications*. Philadelphia, PA: SIAM.

Smith RC and Hu Z (2012) The homogenized energy model for characterizing polarization and strains in hysteretic ferroelectric materials: material properties and uniaxial model development. *Journal of Intelligent Material Systems and Structures* 23(16): 1833–1867.

Sobol' IM (1993) Sensitivity analysis for non-linear mathematical models. *Mathematical Modeling & Computational Experiment* 1: 407–414.

Sobol' IM (2001) Global sensitivity indices for nonlinear mathematical models and their Monte Carlo estimates. *Mathematics and Computers in Simulation* 55: 271–280.

Sobol' IM, Tarantola S, Gatelli D, et al. (2001) Estimating the approximation error when fixing unessential factors in global sensitivity analysis. *Reliability Engineering & System Safety* 92(7): 957–960.

Song HJ, Choi YT, Wereley NM, et al. (2010) Energy harvesting devices using macro-fiber composite materials. *Journal of Intelligent Material Systems and Structures* 21(6): 647–658.

Uchino K (2010) *Ferroelectric Devices*. 2nd ed. Boca Raton, FL: CRC Press/Taylor & Francis.

Uchino K and Giniewicz JR (2003) *Micromechatronics*. New York: Marcel Dekker, Inc.

Vasic D, Sarraute E, Costa F, et al. (2004) Piezoelectric microtransformer based on PZT unimorph membrane. *Journal of Micromechanics and Microengineering* 14: S90–S96.

Weirs VG, Kamm JR, Swiler LP, et al. (2012) Sensitivity analysis techniques applied to a system of hyperbolic conservation laws. *Reliability Engineering & System Safety* 107: 157–170.

Wentworth M, Smith RC and Banks HT (2016) Parameter selection and verification techniques based on global sensitivity analysis illustrated for an HIV model. *SIAM/ASA Journal of Uncertainty Quantification* 4: 266–297.

Wood RJ (2008) The first takeoff of a biologically inspired atscale robotic insect. *IEEE Transactions on Robotics* 24(2): 341–347.

Wood RJ, Finio B, Karpelson M, et al. (2011) Progress on "pico" air vehicles. In: *International symposium on robotics research*, Flagstaff, AZ, 9–12 December, pp. 3–19. Cham: Springer.